BMSAP

Bulletins et mémoires de la société d'anthropologie de Paris
BMSAP

36 (1) | 2024
Analyses invasives, micro-invasives et non-invasives des vestiges anthropobiologiques

Cladistics with geometric morphometric data: The variability of the calvarium in the genus *Homo*

Morphométrie géométrique et cladistique : la variabilité du calvarium du genre Homo

Margaux Simon-Maciejewski, Giorgio Manzi, Valéry Zeitoun et Aurélien Mounier

OpenEdition Journals

Édition électronique
URL : https://journals.openedition.org/bmsap/14053
DOI : 10.4000/bmsap.14053
ISSN : 1777-5469

Éditeur
Société d'Anthropologie de Paris

Référence électronique
Margaux Simon-Maciejewski, Giorgio Manzi, Valéry Zeitoun et Aurélien Mounier, « Cladistics with geometric morphometric data: The variability of the calvarium in the genus *Homo* », *Bulletins et mémoires de la Société d'Anthropologie de Paris* [En ligne], 36 (1) | 2024, mis en ligne le 30 avril 2024, consulté le 07 mai 2024. URL : http://journals.openedition.org/bmsap/14053 ; DOI : https://doi.org/10.4000/bmsap.14053

Cladistics with geometric morphometric data: The variability of the calvarium in the genus *Homo*

Morphométrie géométrique et cladistique : la variabilité du calvarium du genre Homo

Margaux Simon-Maciejewski [1]*, Giorgio Manzi [1], Valéry Zeitoun[2], Aurélien Mounier [3,4,5]

1. Dipartimento di Biologia Ambientale. Sapienza Università di Roma, Rome, Italy
2. UMR 7207-CR2P-CNRS-MNHN-Sorbonne Université, Campus Jussieu, Paris, France
3. Histoire Naturelle de l'Homme Préhistorique (HNHP, UMR 7194) CNRS/MNHN/UPVD, Musée de l'Homme, Paris, France
4. Turkana Basin Institute, Nairobi, Kenya
5. CNRS, UAR 3129 – UMIFRE 11 3 Maison Française d'Oxford, Oxford, United Kingdom

* margauxyveline.simonmaciejewski@uniroma1.it

Reçu : 17 mai 2023 ; accepté : 18 mars 2024
Bulletins et Mémoires de la Société d'Anthropologie de Paris

Abstract – Over the last 30 years, several protocols to adapt 3D geometric morphometric data to cladistics have been developed. Strongly criticised, these protocols are only occasionally used in palaeoanthropology, despite the obvious heuristic potential of such an approach. This study tests two different protocols to analyse 23 operational taxonomic units (OTUs) representing the genera *Pongo*, *Gorilla*, *Pan*, *Australopithecus* and *Homo*, in order to evaluate the phylogenetic information derived from geometric morphometric data. The 23 OTUs were based on averaged Procrustes-aligned coordinates (generalised Procrustes analysis) of three landmark configurations (148, 347 and 636 landmarks) describing the calvarium morphology of 78 specimens. The first protocol used the coordinates of the principal components, obtained after a principal component analysis, as variables describing the OTUs. The second approach directly used the aligned 3D coordinates of the landmarks. These two datasets were then analysed with both the heuristic and branch-and-bound algorithms implemented in the TNT software. These analyses produced a unique cladistic tree for each dataset. Independent of the matrix used to obtain the trees, these preliminary results were phylogenetically consistent and support debated paleoanthropological hypotheses.

Keywords – cladistics, phylogeny, genus *Homo*, geometric morphometric, TNT software

Résumé – Ces 30 dernières années, plusieurs protocoles permettant d'utiliser des données 3D de morphométrie géométrique en cladistique ont été proposés. Fortement critiqués, ces protocoles ne sont qu'occasionnellement utilisés en paléoanthropologie, malgré le potentiel évident d'une telle approche. Dans cette étude, nous avons testé deux protocoles différents afin d'évaluer l'information phylogénétique dérivée des données de morphométrie géométrique, que nous avons appliqué à 23 unités taxonomiques opérationnelles (UTOs) représentant les genres *Pongo*, *Gorilla*, *Pan*, *Australopithecus* et *Homo*. Ces 23 UTOs sont issues de la moyenne des coordonnées procrustes alignées (analyse procruste généralisée) de trois configurations de points-repères (148, 347 et 636 points-repères) décrivant la morphologie du calvarium de 78 spécimens. Le premier protocole utilise les coordonnées des composantes principales, obtenues après une analyse en composantes principales, comme variables décrivant les UTOs. La seconde approche utilise directement les coordonnées 3D alignées des points-repères. Ces deux ensembles de données ont ensuite été analysés à l'aide des algorithmes "heuristic" et "branch-and-bound" implémentés dans le logiciel TNT. Ces analyses ont produit un arbre cladistique unique pour chaque jeu de données. Indépendamment de la matrice utilisée pour obtenir les arbres, ces résultats préliminaires sont phylogénétiquement cohérents et soutiennent des hypothèses paléoanthropologiques intéressantes.

Mots clés – cladistique, phylogénie, genre *Homo*, morphométrie géométrique, logiciel TNT

Introduction

For the past 30 years, virtual imaging has increasingly been applied to non-medical fields of research. Especially in palaeontology and palaeoanthropology (e.g., Balzeau et al., 2012). This methodological revolution has been accompanied by the development of geometric morphometric

methods (GMM, i.e., quantitative analysis that allows to explain and visualise the differences in shape (i.e., form without size) that have been mathematically analysed (Zelditch et al., 2004; Adams et al., 2011). Both methodologies have been adopted by taxonomists and are now widely used to test hypotheses on how to classify specimens of extinct species (Mounier et al., 2011; Mounier, 2012; Profico et al., 2016).

Nevertheless, the rise of these new tools largely ignored a previous methodological improvement in taxonomy: cladistics. Cladistics renewed systematics by introducing in the analysis the concept of ancestor-to-descendant relationships (Matile et al., 1987), while previous taxonomic analyses relied on a phenetic theoretical framework that focused solely on the morphological similarities (Sneath and Sokal, 1973). Morphological data obtained from virtual imaging and geometric morphometrics can be directly analysed within a phenetic theoretical framework but need to be adapted in order to work within a cladistic phylogenetic framework (MacLeod et al., 2002).

Nevertheless, identifying phylogenetic signals from geometric morphometric data has been the focus of several scientific works (MacLeod et al., 2002; Klingenberg and Gidaszewski, 2010) and a few protocols for integrating this type of data into cladistic frameworks have been developed (González-José et al., 2008; Clouse et al., 2011). However, such protocols remain anecdotal, are heavily criticised (Catalano et al., 2010; Adams et al., 2011) and only occasionally used in palaeontology (Smith and Hendricks, 2013). Three main issues are raised by researchers as to why the use of cladistics with GMM should be avoided.

First, should shape data be considered as one trait or as a set of traits, and, if so, how should the partitioning into separate characters or characters' states be performed (Bookstein, 1994; MacLeod et al., 2002; Zelditch et al., 2004)? For analytical procedures operating in a phenetic framework, such as neighbour-joining or those based on likelihood (e.g., maximum likelihood), the question of partitioning does not arise, because the phenetic inferences are made on the distances between taxa (Swofford et al, 1996; Felsenstein, 2004), so that the choice of a particular set of shape variables does not affect the result as long as information on the relative positions of taxa within a multidimensional space is used (Klingenberg and Gidaszewski, 2010). Thus, the definition of a trait (i.e., its coding) is not central and the very notion can be abandoned. On the other hand, for cladistic methods based on Wagner's parsimony (i.e., those which only take into account apomorphies (derived) and whose nodes are built on the degree of shared derived traits), the character need to be well-defined and are assumed to be independent from one another. Such is not the case for 3D morphometric data as the landmark coordinates which represent the extracted shape variables cannot be considered as independent of each other and their definition as discrete traits is, at best, debatable. Each landmark does contain morphological information, but the information itself is only revealed when landmarks are associated with each other.

In order to address these questions, several protocols have been tested in the past. One consisted of using partial distortion scores for landmarks that were "identical" between all the specimens/taxa included in an analysis (e.g., Zelditch et al., 1995; 2000). This method was highly controversial (e.g., Bookstein, 1994; 2002; Monteiro, 2000; MacLeod et al., 2002) and was subsequently abandoned (Zelditch et al., 2004), as the choice of data was considered to be too arbitrary. Another approach subdivided the global shape of the analysed operational taxonomic units (OTU) into smaller parts and considered each of these parts as discrete traits (MacLeod et al., 2002; González-José et al., 2008). While this approach mathematically addressed the issue regarding independence of the variables used to perform the cladistic search – the variables in the cladistic analysis are imputed from the coordinates of the mathematically independent Principal Components (PCs) obtained after a Principal Component Analysis (PCA) –, the way each variable was calculated raised additional concerns. Indeed, the global shapes of the OTUs were divided into shape blocks which were aligned separately through multiple Generalised Procrustes Analyses (GPA). Unfortunately, this creates distortion in the database, as the PCs are derived from several GPAs and PCAs (Adams et al., 2011; Klingenberg and Gidaszewski, 2010). The use of uncorrelated shape variables, as can be obtained from PCA based on terminal taxa (González-José et al., 2011; MacLeod et al., 2002), has also been criticised, as the covariation between terminal taxa is generally not the same as the covariation between evolutionary changes in conformational variables (Felsenstein, 1985; 2004).

While the issue of trait definition and independence is at the root of many controversies surrounding the use of morphometric data (Rohlf, 1998; Monteiro, 2000; Bookstein, 2002), it should be noted that it is also a problem when using "traditional" discrete morphological character because their definitions vary widely (e.g., Thiele, 1993) as it is often difficult to assess their independence (e.g., MacLeod et al., 2002; Mounier et al., 2009).

Finally, according to Adams et al. (2011), methods consisting of forcing multivariate shape variables into a form compatible with cladistic software (Zelditch et al., 1995; Gonzalez-Jose et al., 2008) would distort the information present in these variables and this would severely limit the useful biological conclusions that can be made. This is in fact the case for all implementations of discontinuous coding from a continuous dataset and is therefore not specific to geometric morphometric data.

In order to further contribute to this long-lasting debate, the present study tests two additional protocols that could help to merge the methodological strengths of both approaches: geometric morphometrics to describe and analyse morphological variations, with the aim to infer taxonomy and phenetic relationships from 3D morphological data, and cladistics to reconstruct phylogenies. These methodological procedures aim at analysing a large corpus of 3D data describing the calvarium (i.e., the skull without

the mandible and upper face) of specimens belonging to the genera *Pongo*, *Gorilla*, *Pan* and *Homo*, while addressing the methodological concerns raised in the past regarding cladistics based on geometric morphometric data. More specifically, the first procedure uses PC coordinates as variables for the cladistic analyses obtained from a unique GPA alignment of the OTU 3D coordinates, hence addressing both criticisms regarding mathematical independence of the variables used as traits and the distortion of the database due to multiple GPA alignments. Another raised issue – distortion of the morphological information of the data due to the transformation of multivariate shape variables into a form compatible with cladistic software – is also addressed in the present study, as the TNT software used was developed to accommodate different types of continuous data, including 3D morphometric data (Goloboff et al., 2008).

Finally, additional possible issues regarding the use of GMM in cladistics will be considered through a comparison of the first protocol with a second approach, using the 3D coordinates as variables, and with results from "traditional" numerical taxonomic methods, neighbour-joining and UPGMA, allowing the evaluation of the methodological limitations and strengths of the different protocols.

Materials and Methods

Nature of the data

The 3D models were obtained by one of the authors (AM) through three different procedures depending on the availability of the equipment/specimens: 1) medical computed tomographic scans processed in Amira (v5.5, FEI); 2) photogrammetry using the software Metashape (v1.8.1); and 3) 3D surface scans using an optical scanner (HDI Advance, 45µ accuracy, LMI) and the software Flexscan (V.3.3 LMI) (see Supplementary Information table S1).

Landmark Abbreviations	Names of the landmarks
Na	Nasion
Gl	Glabella
Ho	Hormion
Ba	Basion
Br	Bregma
Op	Opisthion
La	Lambda
In	Inion
Zm*	Anterior zygomatic tubercle
Ma*	Mastoïdal
Fmo*	Frontomalare orbitale
Fmt*	Frontomalare temporale
En*	Entoglenoid
As*	Asterion
Po*	Porion
MTMJ*	Maximum depth of the TMJ
It*	Infra-temporale
Fm*	Frontomalare

* Bilateral landmarks / *Points-repères bilatéraux*

Table 1. Summary of the 27 landmarks used in the study and their abbreviations / *Présentation des 27 points-repères utilisés dans l'étude*

The shape of the calvarium was described using landmarks and semi-landmarks, the latter being allowed to slide (Bookstein, 1997), according to three protocols: A) the first contains 27 landmarks and 121 semi-landmarks (figure 1A; table 1); B) the second contains 27 landmarks and 320 semi-landmarks (figure 1B; table 1); and C) the third contains 27 landmarks and 608 semi-landmarks (figure 1C; table 1). Those datasets were collected with the software Landmark (IDAV, Wiley, 2005).

The data used as variables in our study are composed, for the first set of analyses (tables S2, S4 and S6), of all the coordinates of the PCs generated from a PCA (Abdi and Williams, 2010) led on the aligned 3D landmarks (i.e., after GPA) and, for the second set of analyses, of aligned (i.e., after GPA) 3D coordinates of anatomical landmarks describing the morphology of the calvarium of cast and original specimens (tables S3, S5 and S7).

Choice of operational taxonomic units (OTUs)

To implement and test phylogenetic reconstructions based on 3D geometric morphometrics, different taxa belonging to the family Hominidae Gray, 1825 (e.g., Lockwood and Tobias, 1999) were analysed (table S1). The outgroups are composed of three specimens for each of the genera *Pongo*, *Gorilla* and *Pan*. We used female individuals in order to avoid any distortion of the results due to the presence of strongly expressed secondary sexual characters (e.g., the sagittal crest) in some ape males. The 20 other OTU are formed by representatives of the *Homo* and *Australopithecus* genera.

The specimens STS5 ("Mrs. Ples") and STS71 constitute the OTUs corresponding to the species *A. africanus* Dart, 1925. This species was first considered to be the common ancestor of two later hominid taxa, *A. robustus/boisei* and *Homo* according to Tobias (1980). The specimen STS5 has been the subject of much debate, including its taxonomic attribution, with some authors classifying it as *A. africanus* (Lockwood and Tobias, 1999; Villmoare et al., 2015) and others as *A. afarensis* (Clarke, 2008).

Several taxa of the genus *Homo* representing a broad spectrum of morphological and taxonomical variations were selected (table S1). The two specimens KNM-ER 1470 and KNM-ER 1813 form the OTU representing the species *H. habilis* Leakey, Tobias and Napier, 1964 *sensu lato*. The attribution of these two specimens to the same species has been the subject of much debate (Prat, 2022). Indeed, KNM-ER 1470 has been attributed to *H. habilis* (Walker and Leakey, 1978), *H. rudolfensis* Alexeev, 1986 (Zeitoun, 2000; Argue, 2017) and to the genus *Australopithecus* (Walker and Leakey, 1978), while some others conclude it was a sister group of *H. habilis* and *H. rudolfensis* (Groves, 1989). The KNM-ER 1813 skull has sometimes been assigned to the species *A. africanus* (Walker and Leakey, 1978) and *H. ergaster* Groves and Mazák, 1975 (Groves, 1989; Zeitoun, 2000), but is generally classified as *H. habilis* (Lieberman et al., 1996).

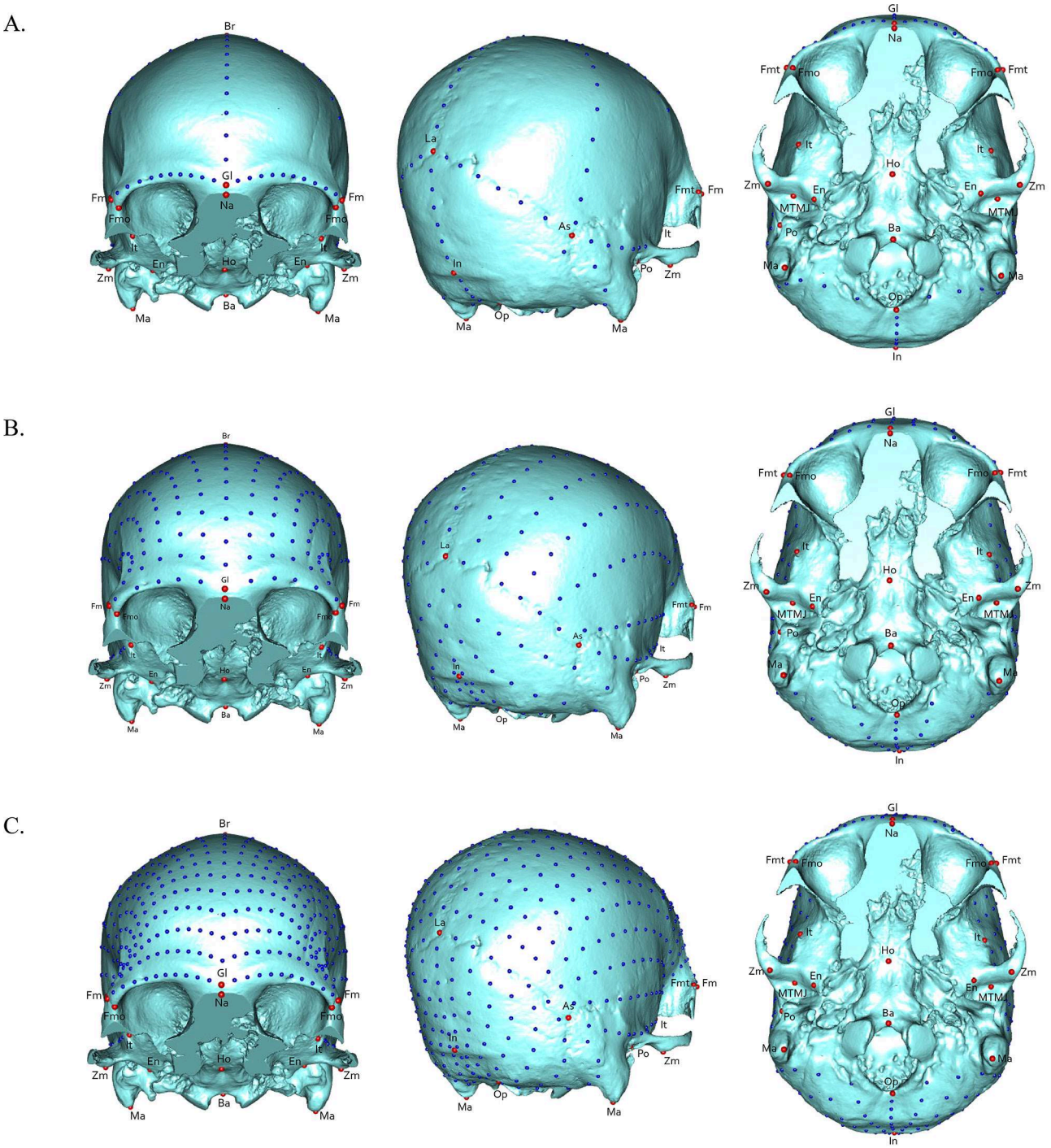

Figure 1. Position of the landmarks on the calvarium for each dataset (A. 148 landmarks; B. 347 landmarks; C. 636 landmarks). From left to right: norma facialis; ¾ view; and norma basalis / *Position des points-repères sur le calvarium pour chaque base de données (A. 148 points-repères ; B. 347 points-repères ; C. 636 points-repères). De gauche à droite : norma facialis, vue de trois-quarts, et norma basalis*

Two specimens from Dmanisi constitute the OTU representing the species *H. georgicus* Gabounia, de Lumley, Vekua and Lordkipanidze, 2002: D2282 and D4500. Analysis of the Dmanisi skulls, particularly that of D4500, has also been used to suggest that some previously recognised species or subspecies within the genus *Homo* correspond to a single evolutionary lineage: *H. erectus* (Lordkipanidze et al., 2013).

Another OTU was formed by combining two specimens, attributed to the species *H. ergaster* Groves and Mazák, 1975: KNM-ER 3733 and 3883. Initially assigned to the species *H. habilis* (White et al., 1981), these specimens were assigned later to *H. erectus* (Walker et al., 1993; Grine et al., 1996) before being incorporated into *H. ergaster* (Groves, 1989; Tattersall, 2013) or even to be affiliated each to two new species (Zeitoun, 2000).

Regarding the species *H. erectus* Dubois, 1893, we used three pairs of specimens belonging to the Sangiran, Sinanthropus and Ngandong series, in order to illustrate the chronological and geographic diversity of this polytypic species. The Ngandong 7 and 14 specimens, first described as belonging to a new species *H.* (*Javanthropus*) *soloensis* by Oppenoorth in 1932, were later assigned to different categories: "archaic" *H. sapiens* or evolved *H. erectus* (Zeitoun, 2000; Zeitoun et al., 2010).

The specimens Sangiran 2 and 17 were initially assigned to the species *Pithecanthropus erectus* Dubois, 1894 by Koenigswald (1940) before being considered archaic *H. erectus* (Sartono, 1982).

Finally, the specimens Sinanthropus III and XI were used. Initially described as belonging to *Sinanthropus pekinensis* Black, 1927, Sinanthropus XI was included later in an *H. sapiens* clade (Zeitoun, 2000) before being affiliated with *H. erectus*.

Regarding the species *H. neanderthalensis* King, 1864, the choice was made to consider taxonomic units that reflect populations recognised as distinct based on genetic data and otherwise belonging to different periods and/or geographical areas (Fabre et al., 2009). Thus, the taxonomic operational unit "early Neanderthal" includes two specimens: Saccopastore 1 and Ehringsdorf H. A "Near East Neanderthal" taxonomic operational unit consists of the specimens Amud 1 and Shanidar 1. The Monte Circeo, La Ferrassie 1 and La Chapelle-aux-Saints specimens constitute the "Classic Neanderthal" taxonomic operational unit.

Finally, to take into account the variability within the species *H. sapiens*, different OTUs have been constituted. The first, called "early sapiens" corresponds to fossil specimens of *H. sapiens*: Qafzeh 6, Qafzeh 9 and Skhül V. Then eight OTUs, composed of five recent individuals each, were formed in order to reflect the evolutionary history of human populations as indicated by the genetic diversification between different metapopulations (table S1) (Mounier and Mirazón Lahr, 2016).

A total of 78 specimens were used in the study. We chose to run the cladistics analysis at the populational/species level, therefore the shape describing the specimens included in the study were averaged per populations/species (see "Modality of data processing") to form the 23 operational taxonomic units of the cladistic analyses.

Modality of data processing

We estimated the position of missing landmarks, by mirroring the existing landmarks onto the other side and, when not possible, by estimating them by thin-plate-spline interpolation (i.e., TPS, Bookstein, 1989). Then, the 78 landmark configurations containing 636 landmarks describing our samples were aligned using GPA (Gower, 1975; Rohlf and Slice, 1990; Goodall, 1991) and bilateral asymmetry was removed from the data (Klingenberg et al., 2002). The 23 OTUs (including the three outgroups) were then computed as an average of the specimens forming each group described above and six different matrices were calculated. Matrices A.1 (table S2) and A.2 (table S3) were based on the analysis of 148 landmarks. Matrix A.1 used the PC coordinates for each OTU obtained after running a PCA on the Procrustes residuals resulting from the alignment of the 23 averaged configurations (table S2). Matrix A.2 was directly formed with the Procrustes-aligned 3D coordinates of the 148 landmarks averaged per OTU (table S3). Matrices B and C were based on 347 and 636 landmarks respectively. The same protocol used for the above configuration of 148 landmarks was applied to matrices B and C: B.1 (table S4) and C.1 (table S6) use the PC coordinates obtained after GPA and PCA, while B.2 (table S5) and C.2 (table S7) directly use the aligned 3D coordinates of the landmark describing each OTU. Variables presenting negative values cannot be processed by TNT software version 1.5 (Goloboff and Catalano, 2016). The protocol using the PC coordinates present negative values and to allow the software to process the data and perform the analysis, we added ten units to each variable of the three matrices. To verify that the order of the taxa did not impact the results several analyses were performed with different outgroups, changing the order of the taxa in the matrix.

Phylogenetic analysis of the data and choice of options

While the current debate on the use of geometric morphometric data in cladistics remains open, few technical means are available to test the approach implemented here. Among all the available cladistic software (e.g., PAUP*, Hennig68), only TNT of the Willi Hennig Society presents algorithms allowing the direct use of continuous (overlapping) quantitative data. These algorithms will attempt to reconstruct ancestral trait states by establishing the shape, estimated from landmarks, with the goal of parsimoniously minimising the morphological evolution of the tree based on optimisation logic (Catalano et al., 2010; Goloboff and Catalano, 2011; Ascarrunz et al., 2019; 2021).

The approach used here is that of Goloboff and Catalano (2010; 2011). It operates directly on the coordinates of the PCs or of those of the landmarks, attempting to

minimise the individual displacement of landmarks between ancestors and descendants. To do this, it will estimate the ancestral configurations at internal nodes in a manner analogous to the estimates of trait states in traditional parsimony, i.e., with discrete (non-overlapping) qualitative data. The ancestral patterns will be "spatial" and the coordinates of the landmarks will be optimised as a multivariate trait. The protocol aims to find the ancestral position of a landmark, by trying a limited set of positions determined by a grid encompassing the range of observed landmark positions in descendants. The ancestral position can be refined by increasing the number of grid subdivisions or by repeating the procedure using a smaller grid around the position of the first approximation.

Therefore, six parsimony phylogenetic analyses were run, one for each of the protocols for both matrices. The use of new samples of landmarks for matrices B and C was driven by the need to best describe the morphology of the calvarium, while addressing possible technical problems, such as the limit of the number of analysable landmarks by the TNT software and a prohibitive computational time above a certain number of landmarks. Indeed, the parsimony analysis of the second protocol of matrix C could not be completed as the high number of variables (i.e., 636 landmarks) is beyond the computational capacity of the TNT software. In each case, 20 OTUs formed the ingroup (the genera *Homo* and *Australopithecus*) and three OTUs served as outgroups (the genera *Gorilla*, *Pan* and *Pongo*) to root the search and polarise the transformations of the variables. Phylogenetic analyses were performed with TNT version 1.5 parsimony software (Goloboff and Catalano, 2016), allowing the comparison of multiple hypotheses of relatedness and the quick selection of the most parsimonious. Parsimony has been chosen because it is the only phylogenetic reconstruction method that allows for the identification and discussion of the number and nature of synapomorphies observed at individual nodes (Matile et al., 1987).

In the analyses presented here, characters were treated in an unordered manner and no transformation cost matrix was applied. The analyses of the matrices were performed with a heuristic algorithm, with random addition sequence (RAS), and tree bisection and reconnection (TBR) branch swapping, i.e., the tree is split into subtrees, which are then moved and reconnected to each other until the final tree, with the least number of steps, is found.

The consistency index (CI) gives us an idea on the robustness of the trees with an indication of the degree of homoplasy present in each tree. However, if the number of autapomorphies is high in a tree, this index value will be high (tending towards 1), regardless of the homoplasy content of the other traits. To solve this issue, we also calculated the retention index (RI), which represents the ratio between the maximum number of homoplasies observed and the number of homoplasies that can be observed.

In the case of the first protocol (analyses A.1, B.1 and C.1), a weighting of the variables, using the RIs of each PC, was applied before running a subsequent tree search, which used a non-exhaustive exact "Branch and Bound" algorithm, guarantying an optimal solution (Mounier and Caparros, 2015). The pre-variable RI gives information about the presence or absence of phylogenetic information, i.e., an RI=1 indicates the presence of a synapomorphy, on the opposite an RI=0 represents a homoplasic character (Farris, 1989).

The robustness of each of the branches was finally evaluated via 100 bootstrap replications (following Felsenstein, 1985).

Results

The morphological variation present in the initial data sets (i.e., with configurations of 148, 347 and 636 landmarks) was first explored at the level of individual specimens using PCA analyses (table S8). In the resultant morphospaces, specimens occupy positions consistent with their usual taxonomic assignment in palaeoanthropology (tables S9-S11). When the average landmark configurations (i.e., used as variable for the OTUs) were used to compute the PCAs, the morphospaces described by PCs 1 to 3 indicate, as expected, an even stronger pattern of taxonomic groupings than what could be observed initially (tables S12-S14).

The initial heuristic search on analyses A.1, B.1 and C.1 (i.e., composed of 22 PCs) resulted in several trees (figures 2-4; tables S15-S17). Out of the 22 PCs, three presented a RI superior to 0.35 for matrix A (figure 5), six PCs for matrix B (figure 6) and four PCs for matrix C (figure 7).

For analysis A.1, heuristic analysis at 200 replications – i.e., the construction of the Wagner tree (the most parsimonious tree) and the application of TBR branch-swapping are replicated 200 times independently – produces two equally parsimonious trees that differ in the relationships between the modern human populations and in the positions of *H. habilis*, *H. ergaster* and Sinanthropus (table S15, node U of figure 5). Both trees are 2,630 steps long with a CI of 0.422 and a RI of 0.575 (table S15). After reweighting the 22 PCs using the RI values of each trait, a subsequent Branch-and-Bound analysis produces a single tree of 931,403 steps (CI=0.569 and RI=0.806) (figure 2A). The heuristic analysis of matrix B.1 results in three equally parsimonious trees of 2.456 steps, with a CI of 0.437 and a RI of 0.576 (table S16). After reweighting the 22 characters using the RI values and submitting them to a Branch-and-Bound analysis, we obtain a unique tree of 968.626 steps (CI=0.561 and RI=0.771) (figure 3A). Heuristic analysis of matrix C.1 results in two equally parsimonious trees of 2,384 steps with a CI of 0.443 and a RI of 0.57 (table S17). After reweighting the 22 traits using the RI values, a Branch-and-Bound analysis generates a unique tree of 915,513 steps (CI=0.575 and RI=0.781, figure 4).

Analysis A.2, corresponding to 148 landmarks, results in a unique tree of 2.65227 steps (figure 2B), with a CI of 0.468. Nevertheless, the RI could not be computed in TNT and is, therefore, unknown. Analysis B.2, i.e., 347 landmarks, results in a unique tree of 2.70438 steps (figure 3B)

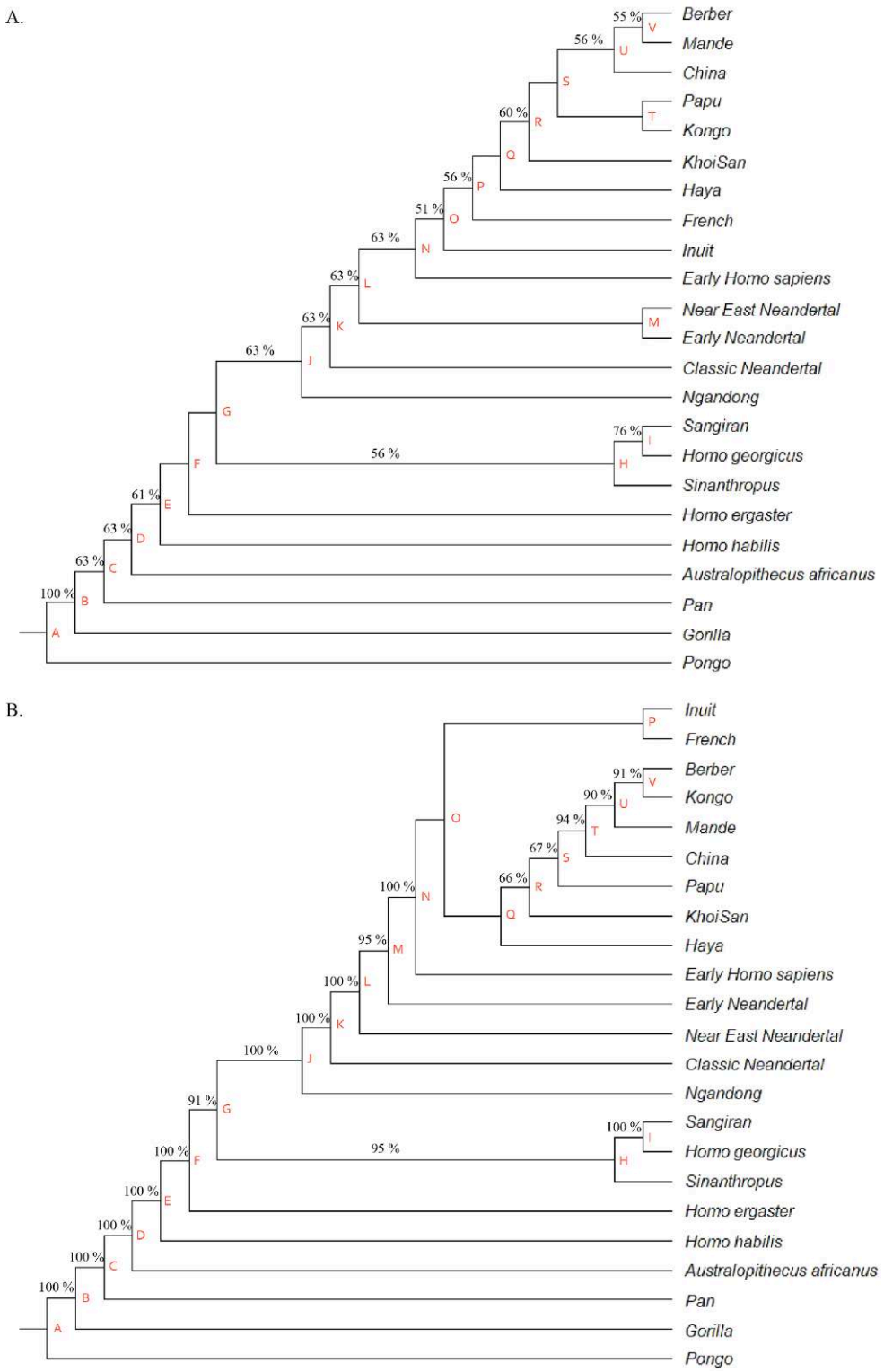

Figure 2. Parsimony phylogenetic trees based on a configuration of 148 landmarks: A) Matrix A.1 analysis of 22 PC coordinates resulting in a unique tree (2,630 steps, CI=0.569 and RI=0.806); B) Matrix A.2 analysis of the aligned 3D coordinates of the landmarks resulting in a unique tree (2,65227 steps and CI=0.468). Values shown above the branches represent bootstrap scores over 100 replications (node values below 50% are not shown). Red letters are used to name the nodes / *Arbres phylogénétiques les plus parcimonieux, basés sur l'analyse de la conformation de 148 points-repères : A) Arbre unique (2,630 pas, et IC=0,468) issu de l'analyse de la matrice A.1 (coordonnées des 22 CPs) ; B) Arbre unique (2,65227 pas, IC=0,468 et IR=0806) issu de l'analyse de la matrice A.2 (coordonnées alignées des points-repères) Les valeurs indiquées sur les branches représentent les scores de bootstrap après 100 réplications (les valeurs inférieures à 50 % ne sont pas montrées). Les lettres rouges correspondent aux noms des nœuds*

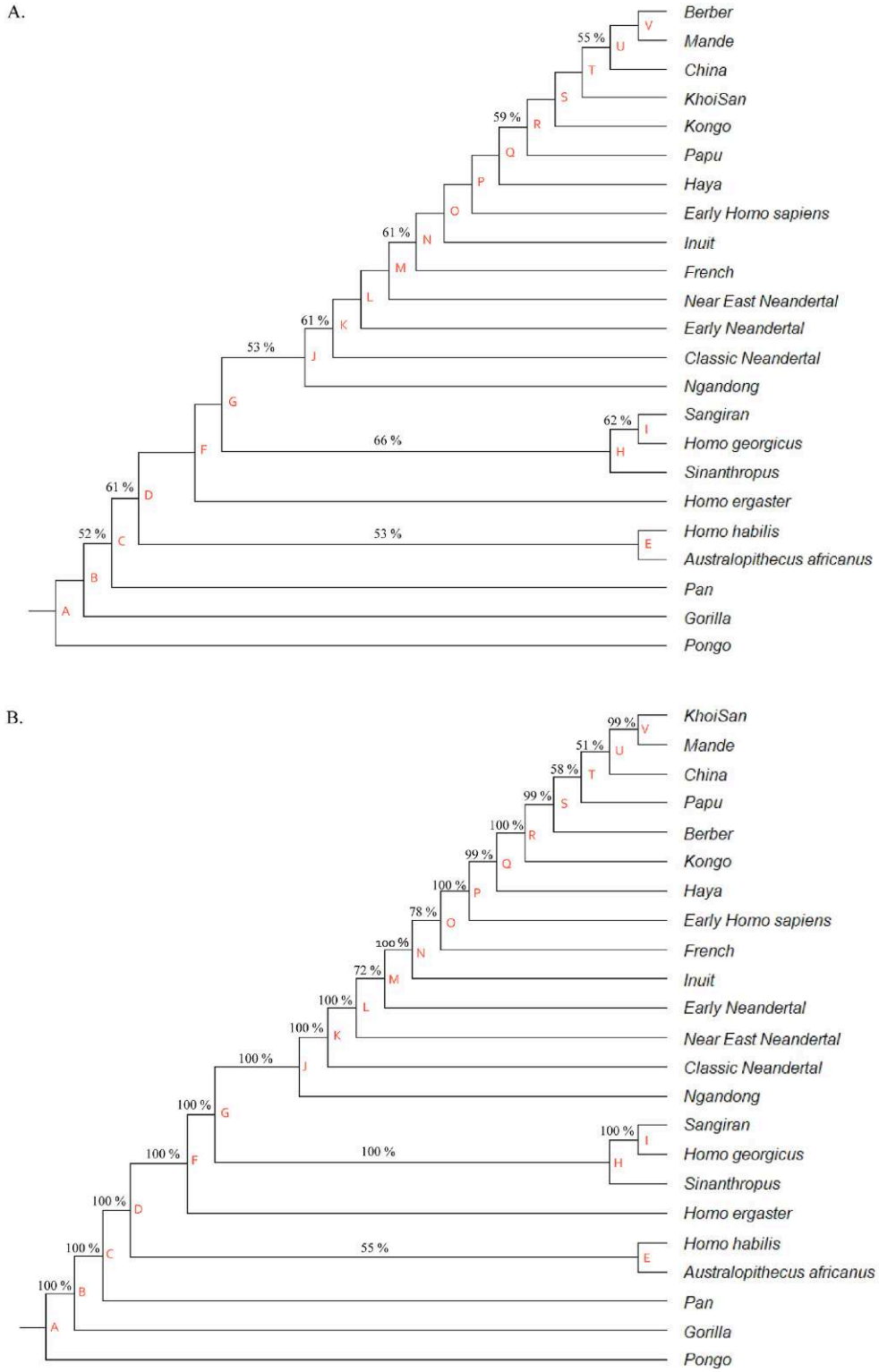

Figure 3. Parsimony phylogenetic trees based on a configuration of 347 landmarks: A) Matrix B.1 analysis of 22 PC coordinates resulting in a unique tree (968,626 steps, CI=0.561 and RI=0.771); B) Matrix B.2 analysis of the aligned 3D coordinates of the landmarks resulting in a unique tree (2,70438 steps and CI=0.468). Values shown above the branches represent bootstrap scores over 100 replications (node values below 50% are not shown). Red letters are used to name the nodes / *Arbres phylogénétiques les plus parcimonieux, basés sur l'analyse de la conformation de 347 points-repères : A) Arbre unique (968,626 pas, IC=0,561 et IR=0,771) issu de l'analyse de la matrice B.1 (coordonnées des 22 CPs) ; B) Arbre unique (2,70438 pas, IC=0,468) issu de l'analyse de la matrice B.2 (coordonnées alignées des points-repères) Les valeurs indiquées sur les branches représentent les scores de bootstrap après 100 réplications (les valeurs inférieures à 50 % ne sont pas montrées). Les lettres rouges correspondent aux noms des nœuds*

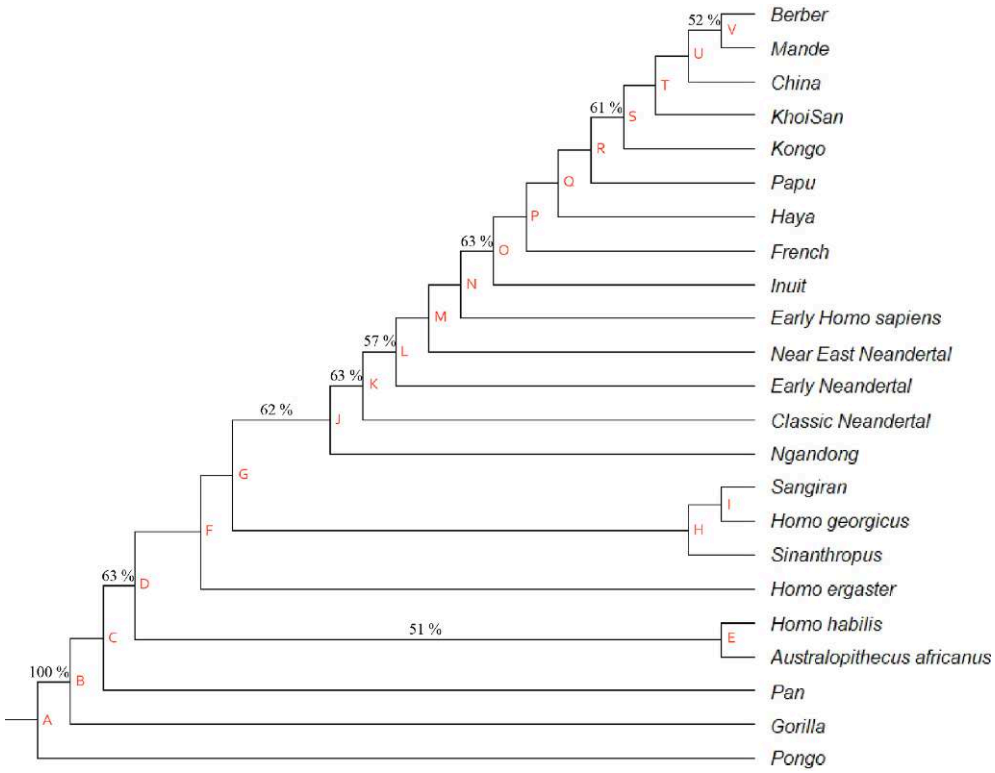

Figure 4. Parsimony phylogenetic tree (931,203 steps, CI=0.575 and RI=0.781) based on the analysis of a configuration of 636 landmarks. Only the analysis of matrix C.1 (22 PC coordinates) yielded results. The values shown above the branches represent bootstrap scores over 100 replications (node values below 50% are not shown). Red letters are used to name the nodes / *Arbre phylogénétique le plus parcimonieux (931,203 pas, IC=0,575 et IR=0,781), basé sur l'analyse de la conformation de 636 points-repères. Seule l'analyse de la matrice C.1 (coordonnées de 22 CP) a permis d'obtenir des résultats. Les valeurs indiquées sur les branches représentent les scores de bootstrap après 100 réplications (les valeurs inférieures à 50% ne sont pas montrées). Les lettres rouges correspondent aux noms des nœuds*

with a CI of 0.468. Finally, the heuristic analysis C.2, corresponding to the 636 landmarks, could not be processed by TNT (see Methods). While matrices with several million characters, such as genomic sequences, have been processed successfully before (Torres et al., 2022), the use of landmarks has been found to be currently limited to 541.

The unique most parsimonious tree resulting from the two-step analysis of matrix A.1 tree (figure 2A) shows that, at node D, the shift towards a value of -0.1 in PC1 explains the formation of the node. Node H supports a monophyletic group composed of the series: Sinanthropus, Sangiran and *H. georgicus*. Sangiran and *H. georgicus* constitute a terminal clade at node I. At node H, it is the values greater than -0.042 in PC1 and less than -0.012 in PC2 that explain the formation of the node. The Neanderthals appear as a paraphyletic group, but the Near East Neanderthal and the earliest early Neanderthal forms are grouped into one clade. At node M, the shift to a value of 0.02 in PC1 explains the formation of the node. At node N – i.e., the OTUs belonging to *H. sapiens* ("early *H. sapiens*" and the various modern human populations today) –, it is the shift to values greater than 0.025 in PC1 and -0.013 in PC2 that explain the formation of the node.

In the tree from the A.2-matrix analysis (figure 2B), the monophyletic group including Sinanthropus and Sangiran/*H. georgicus* at nodes H and I is supported by bootstrap values of 95% and 100%, respectively. The monophyletic *H. sapiens* group appears at node N, with a bootstrap score of 100%. In contrast, Neanderthals also appear as a paraphyletic group.

The unique most parsimonious tree resulting from the two-step analysis of matrix B.1 tree (figure 3A) shows that, at node D, the shift towards a value of -0.1 in PC1 explains the formation of the node. Contrary to the tree obtained from matrix A.1, the one obtained with matrix B.1 shows that, at node E, we observe that the taxon *A. africanus* forms a clade with the taxon *H. habilis sensu lato*, supported by a bootstrap of 53%. It is a shift towards a value of 0.25 in PC2 that explains the formation of this node. Node H supports a monophyletic group composed of the series: Sinanthropus, Sangiran and *H. georgicus*. The latter two taxa constitute a terminal clade at node I. At node H and I, it is a value inferior to -0.04 in PC3 and inferior to -0.005 in PC4, respectively, that explains the formation of the nodes. The Neanderthals appear as a paraphyletic group. At node N, i.e., the OTUs belonging to *H. sapiens* ("early

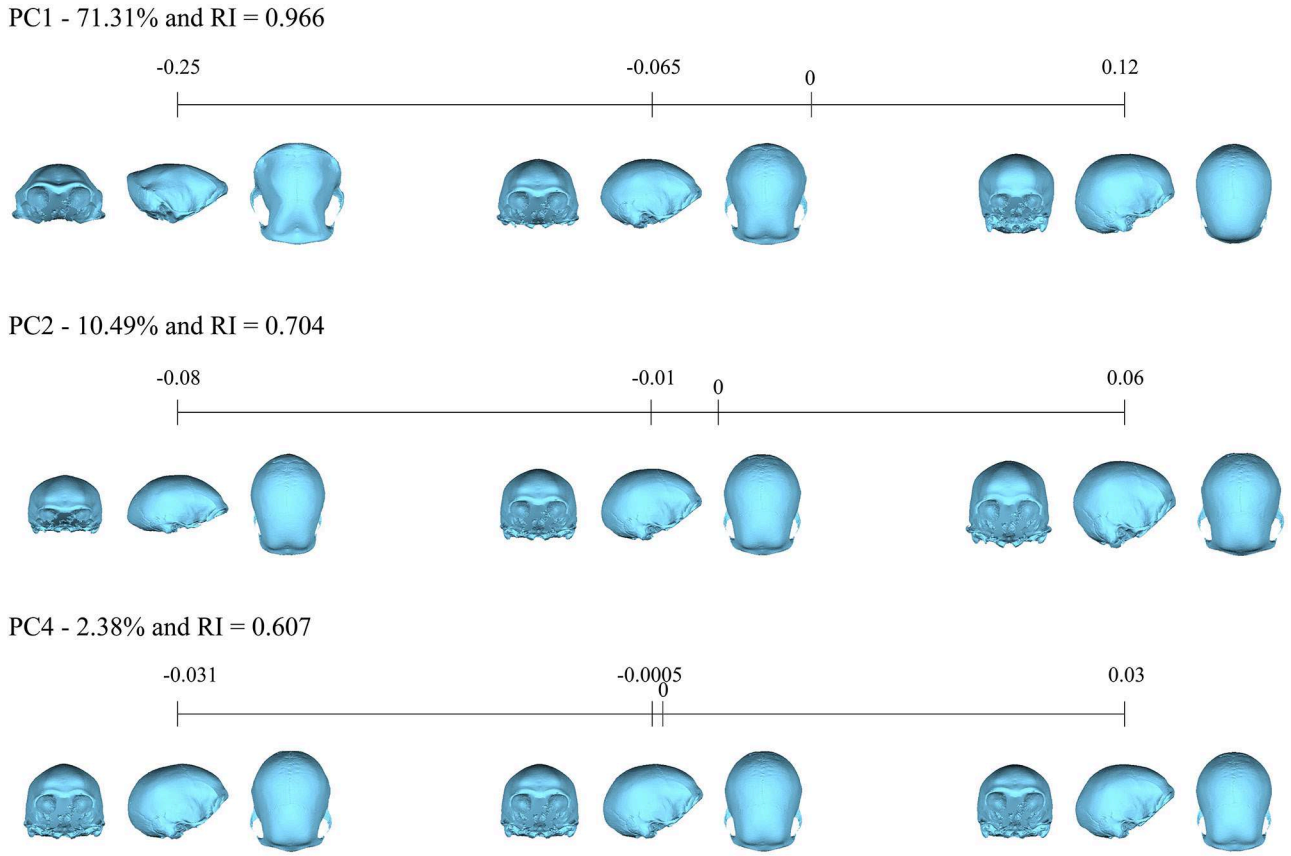

Figure 5. Cranial deformations represented by PCs obtained from the analysis of 148 landmarks. Only PCs with RI≥0.35 are shown. Values shown in percent represent variance / *Déformations crâniennes représentées par les composantes principales (CP) obtenues après l'analyse de 148 points-repères. Seules les CP présentant une valeur de IR≥0.35 sont représentées. La variance de chaque CP est representée en pourcentage*

H. sapiens" and the various modern human populations today), it is the shift to values greater than 0.04 in PC1 and -0.025 in PC2 that explains the formation of the node.

In the tree from the B.2-matrix analysis (figure 3B), the monophyletic group including Sinanthropus and Sangiran/*H. georgicus* at nodes H and I is supported by bootstrap values of 100% in each case. The monophyletic *H. sapiens* group appears at node N, with a bootstrap score of 100%. In contrast, Neanderthals also appear as a paraphyletic group. During the bootstrap analyse, the formation of a clade *A. africanus*/*H. habilis*, with a bootstrap of 55%, can be observed.

As with the tree obtained from matrix B.1, the one obtained with matrix C.1 (figure 4) also shows that, at node E, the clade composed with the taxon *A. africanus* and *H. habilis sensu lato*, is supported by a bootstrap of 51%. It is the shift to a value of 0.029 in PC2 which explains the formation of the *A. africanus* and *H. habilis* clade, while the other taxa keep a value less than 0.029. At node D, the shift towards a value of -0.05 in PC1 explains the formation of the node. On the other hand, we find the same Sinanthropus and Sangiran/*H. georgicus* clade at nodes H and I, supported respectively by bootstraps of 56% and 76%. At node H, it is a value smaller than -0.03 on PC3 that explains the formation of the node. The Neanderthals appear as a paraphyletic group. At node N, i.e., the OTUs belonging to *H. sapiens*, it is the shift to a value of 0.03 in PC1 which explains the formation of the node.

Regarding the morphological changes associated with the nodes of the tree obtained from matrix A.1 (figures 2A and 5), at node D, it is the shift towards a value of -0.1 on PC1 that explains the formation of the node. This translates into various anatomical changes: the cranial outline in *norma occipitalis*, the definition of which depends on the position of the greatest cranial width (bi-euryon), is of triangular shape ("tent-like") (Grimaud, 1982); the post-orbital constriction is less marked compared to the one observed in apes; in *norma verticalis*, the profile of the supraorbital area goes from concave in its medial part at the level of the *glabella* to rectilinear; in *norma lateralis*, the profile of the antero-posterior frontal bone is more convex than the one of apes; and in *norma lateralis*, the transition between the *planum occipital* and the *planum nucale* is rounded, compared to the angular one of apes. At node H and I, it is values greater than -0.042 on PC1 and less than -0.012 on PC2 which explain the formation of the node regrouping *H. erectus* (Sinanthropus and Sangiran) and *H. georgicus*. This shows that the cranial outline in

norma occipitalis is of triangular shape ("tent-like") (Grimaud, 1982) compared to that of Neanderthals, for whom it is circular ("bomb-like" shaped) (Boule, 1911; 1912; 1913; Vandermeersch, 1981; Condemi, 1992); in *norma verticalis*, the profile of the supraorbital area goes from rectilinear for Sinanthropus to concave for Sangiran and *H. georgicus*; and in *norma lateralis*, the angle between the *planum occipital* and the *planum nucale* is more salient, compared to the other OTUs; we can also observe the fusion of the supraciliary arches in the medial portion of the supraorbital area. In this tree, the Neanderthals appear as a paraphyletic group, with the particularity that the Near East Neanderthal and the early Neanderthal are grouped into one clade. At node M, the shift to a value of 0.02 on PC1 explains the formation of the node. This shows that the cranial outline in *norma occipitalis* is more similar to that of *H. sapiens*, for whom it is pentagonal ("house-like") (Broca, 1868; Olivier, 1960), than to that of the "classic Neanderthal" OTU which presents a circular shape ("bomb-like") (Boule, 1911; 1912; 1913; Vandermeersch, 1981; Condemi, 1992); in *norma verticalis*, the profile of the supra-orbital region is convex and does not present the concavity in its medial part at the level of the *glabella*; in *norma lateralis*, the convexity of the antero-posterior frontal bone is more convex than for the "classic Neanderthal" OTU, but not as much as that of *H. sapiens*; and in *norma lateralis*, the angle formed by the *planum occipital* and the *planum nucale* is almost absent. The grouping of early and Near East Neanderthal could correspond to morphological similarity between the oldest Neanderthals whose morphology may not yet show the complete Neanderthal morphological pattern and others that show a slightly different morphotype, closer to the complete Neanderthal morphological pattern (Hublin, 1998). The N-node supports the grouping of all *H. sapiens*: "early *H. sapiens*" and the various modern human populations today. At this node, it is the shift to values greater than 0.025 on PC1 and -0.013 on PC2 that explain the formation of the node. This means that the cranial outline in *norma occipitalis* is pentagonal shape ("house-like") (Broca, 1868; Olivier, 1960); in *norma verticalis*, the profile of supra-orbital region is convex; in *norma lateralis*, the convexity of the antero-posterior frontal bone is very pronounced; and in *norma lateralis*, the angle between the *planum occipital* and the *planum nucale* is totally absent.

As for the morphological traits of the tree of matrix B.1 (figures 3A and 6), at node D, it is the shift towards a value of -0.1 in PC1 that explains the formation of this node. The morphological changes indicated by this value are, for the most, similar to those observed on the matrix A.1 tree: the cranial outline will present the same shape; the post-orbital constriction is also less marked compared to the one observed in apes; in *norma verticalis*, the profile of the supraorbital area goes from concave to rectilinear in its medial part at the level of the *glabella*; in *norma lateralis*, the convexity of the antero-posterior frontal bone is more convex than the one of the great apes; and in *norma lateralis*, the angle between the *planum occipital* and the *planum nucale* is similar to the one observed in the matrix A.1 tree. At node E, it is the shift to a value of 0.25 on PC2, which explains the formation of the *A. africanus* and *H. habilis* clade. This indicates that the cranial outline in *norma occipitalis* presents a more accentuated triangular shape ("tent-like") (Grimaud, 1982) than the rest of the OTUs; the post-orbital constriction is important compared to the other specimens; in *norma verticalis*, the profile of the supraorbital area goes from rectilinear for *H. habilis* to convex for *A. africanus*; and in *norma lateralis*, the angle between the *planum occipital* and the *planum nucale* is more rounded, compared to the strong angle observed in *H. ergaster*. At node H and I, it is values greater than -0.04 on PC3 and less than -0.005 on PC4 respectively, which explain the formation of the node regrouping *H. erectus* (Sinanthropus and Sangiran) and *H. georgicus*. In this tree, the Neanderthals appear as a paraphyletic group, with the disappearance of the Near East and early Neanderthal clade. As for node N, supporting the grouping of all *H. sapiens*, i.e., "early *H. sapiens*" and the various modern human populations, it is the shift to values greater than 0.04 on PC1 and -0.025 on PC2 that explain the formation of the node. The morphological characteristics of this node are very similar to those from the preceding trees. We can observe the same pentagonal shape for the cranial outline in *norma occipitalis*; in *norma verticalis*, the profile of the supraorbital area will also be convex; in *norma lateralis*, the convexity of the antero-posterior frontal and the angulation between the *planum occipital* and the *planum nucale* are identical to those formerly observed in tree A.1.

As mentioned above, the tree obtained from matrix C.1 is very similar to those of matrices A.1 and A.2. In the tree of matrix C.1 (figures 4 and 7), except for some minor changes in the *H. sapiens* clade, there is only the presence of the node *A. africanus*/*H. habilis* (as in matrix B.1, figure 3A) and the absence of the clade Near East/early Neanderthal (in contrast with matrix A.1, figure 2A). At node D, it is the shift to a value of about -0.05 on PC1 that explains the formation of the node. The distribution of morphological characteristics is similar to those of the other trees. At node E, the shift to a value of 0.29 on PC2 explains the formation of the *A. africanus* and *H. habilis* clade. This references the same characteristics as those of node E in the matrix B.1 tree: the cranial outline in *norma occipitalis* is in a more accentuated triangular shape ("tent-like") (Grimaud, 1982) than in the rest of the OTUs; the post-orbital constriction is important compared to the other specimens; in *norma verticalis*, the profile of the supraorbital area goes from rectilinear for *H. habilis* to convex for *A. africanus*; and in *norma lateralis*, the transition between the *planum occipital* and the *planum nucale* is more rounded, compared to the angle in *H. ergaster*. At nodes H and I, it is a value inferior to -0.03 on PC3, which explains the formation of the node regrouping *H. erectus* (Sinanthropus and Sangiran) and *H. georgicus*. The morphological traits for those two nodes are similar to those described for the

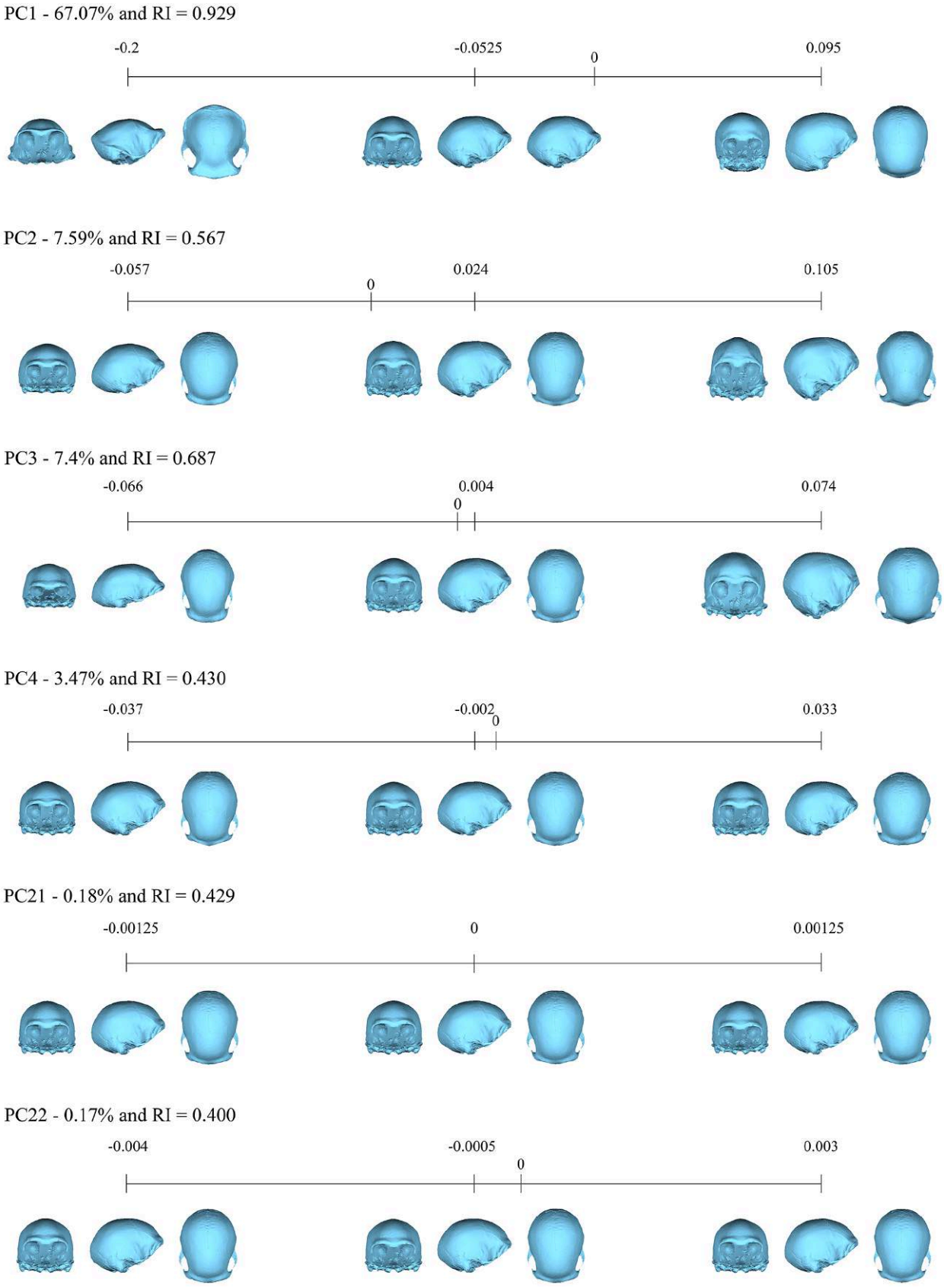

Figure 6. Cranial deformations represented by PCs obtained from the analysis of 347 landmarks. Only PCs with RI≥0.35 are shown. Values shown in percent represent variance / *Déformations crâniennes représentées par les composantes principales (CP) obtenues après l'analyse de 347 points-repères. Seules les CP présentant une valeur de IR≥0.35 sont représentées. La variance de chaque CP est representée en pourcentage*

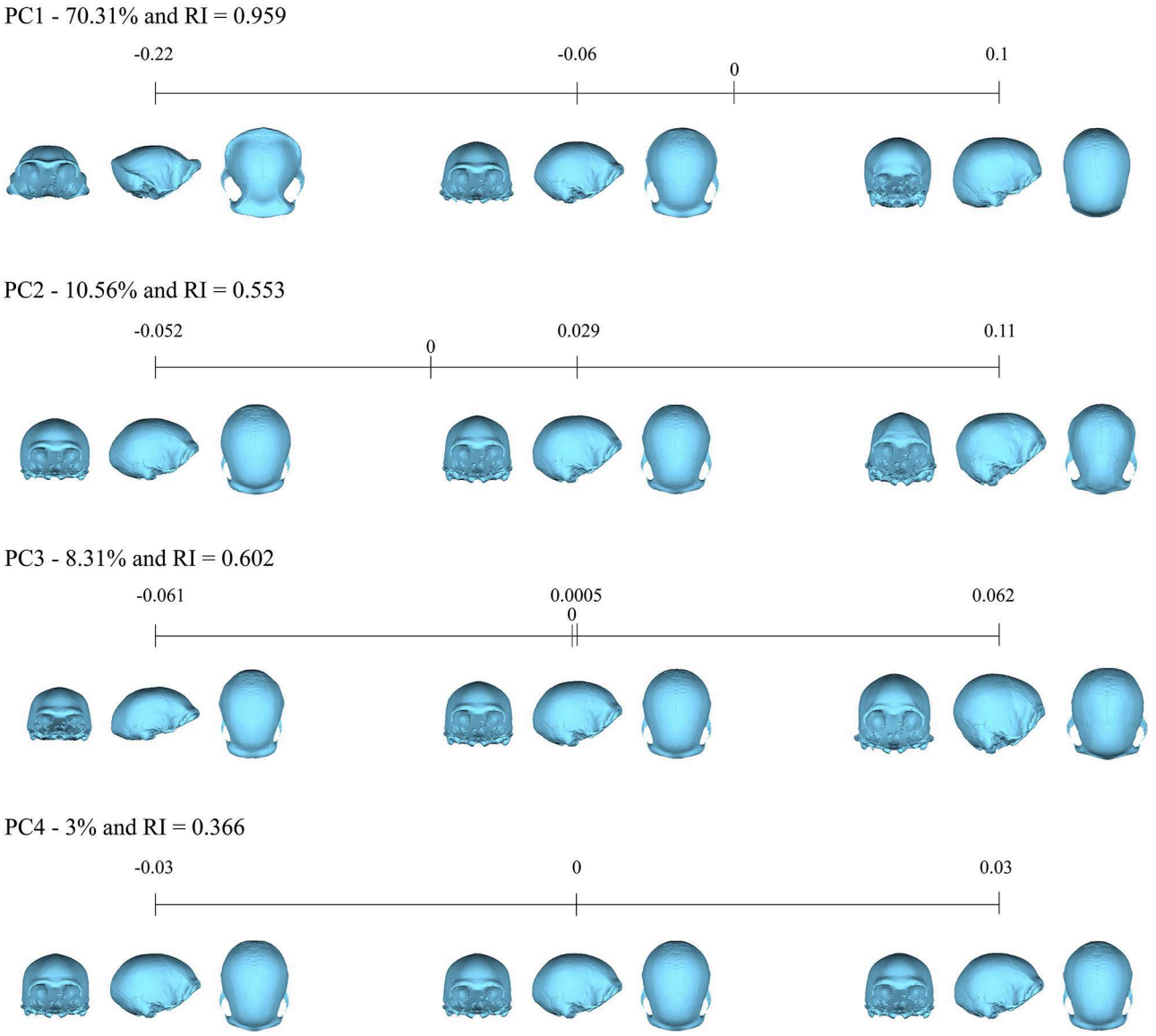

Figure 7. Cranial deformations represented by PCs obtained from the analysis of 636 landmarks. Only PCs with RI≥0.35 are shown. Values shown in percent represent variance / *Déformations crâniennes représentées par les composantes principales (CP) obtenues après l'analyse de 636 points-repères. Seules les CP présentant une valeur de IR≥0.35 sont représentées. La variance de chaque CP est representée en pourcentage*

former trees including the same clade. In this tree, the Neanderthals still appears as a paraphyletic group, but, as in the B.1-matrix tree, the Near East Neanderthal and the early Neanderthal are not grouped into one clade. In node N, i.e., supporting the grouping of all *H. sapiens*, it is the shift to a value of 0.03 on PC1 which explains the formation of the node, with morphological characteristics similar to those allocated to *H. sapiens* (e.g., a globular braincase; a short and high cranium; a long and high parietal arch; a high frontal arch; a rounder frontal bone; etc.).

In this study, the CI and RI indices of the parsimony trees in matrices A.1, B.1 and C.1 are relatively high and reflect a robust phylogenetic signal. However, the RI for the matrix A.2 tree could not be obtained despite several attempts, and the literature does not explain this either.

Discussion

The main objective of this study was to test different protocols to combine 3D geometric morphometrics and cladistics. We ran several analyses using different types of data: coordinates of shape PCs and 3D coordinates of aligned landmark configurations.

Such methodological approaches raise questions regarding inherent technical constraints in carrying out these analyses. First, these issues will be addressed, before focusing on the palaeoanthropological implications raised by the results of the present study, including the impact that the initial step of grouping the specimens into morphometric combinations designed to form OTUs may have had on the interpretation of the phylogenetic hypotheses that have been formulated.

The methodology also presents biases related to several constraints that appeared in the processing of the information and the exploitation of morphometric units taken as OTUs of different taxonomic ranks. For analysis 1 (A.1, B.1 and C.1), the reduction of dimensionality through a PCA transformed the original variables into independent, orthogonal variables, at least from a mathematical point of view, thus, addressing possible problems linked to trait dependency generally present in the case of 3D geometric morphometric data. This issue, nevertheless, remains for the second set of analyses (A.2, B.2 and C.2) which use the correlated untransformed morphological contents as variables (i.e., 3D landmark coordinates). Comparisons of the results obtained from both approaches bring insight into the importance of the definition and the independence of the characters, especially when they can be compared to results obtained through "classical" numerical taxonomy. Indeed, the phylogenies obtained from both cladistic approaches are remarkably congruent and, except for a few differences such as the grouping of *A. africanus* and *H. habilis*, the obtained phylogenies are very similar. Moreover, the phenetic approaches which were tested on the PC coordinate database show a much higher degree of instability, producing a phenetic tree similar to the obtained phylogenies when 148 landmarks are used to describe the calvaria, while the phenetic trees from 347 and 636 landmarks produce very different typologies from the phylogenies (tables S19, S20). Therefore, and despite the possible theoretical issues related to using 3D geometric morphometric data in a cladistic framework, the obtained results in the present study, clearly indicate that the cladistic analysis better handles large 3D databases than classic numerical taxonomic approaches.

Regarding the phylogenetic and palaeoanthropological content of the results obtained, firstly, the relative position of the OTUs in the different phylogenetic trees computed from five different matrices (A1, A2, B1, B2 and C1) are both congruent with the established phylogenies/chronologies and with the grouping observed in the morphospaces resulting from the PCA analyses (tables S9-S14), including the position of the outgroups. We can also notice the monophyly of *H. sapiens*, with slight differences in the relationships among modern human populations.

Hence, our results contribute to the discussion regarding long standing debates in palaeoanthropology. For instance, trees B.1 and C.1, computed respectively from the PC coordinates derived from the analyses of 347 and 636 landmark datasets, show the formation of a clade *A. africanus/H. habilis sensu lato*, supported by bootstrap values of 55% and 51%. This result refers to the debate regarding the validity of the species *H. habilis* and its belonging to the genus *Homo* (Stringer, 1986; Prat, 1997). As we explained before, the two specimens forming the present study's OTU of early *Homo*, KNM-ER 1470 and 1813, have seen their taxonomic attribution challenged over the years. While a number of studies are discussing the possibility that these specimens belong to different species of the genus *Homo* (i.e., *H. rudolfensis* and *H. habilis* (see Lieberman et al. 1996; Zeitoun, 2000; Argue, 2017), others question the attribution of these two fossils to the genus *Homo* to begin with and would advocate for their inclusion into the genus *Australopithecus* (Walker and Leakey, 1978; Wood and Collard, 1999). Therefore, the formation of a monophyletic clade *A.* africanus/*H. habilis* could be interpreted as support for the inclusion of the specimens attributed to *H. habilis* into the genus *Australopithecus* (Walker and Leakey, 1978). Alternatively, our results are based on the analysis of an OTU associating two specimens from the same site, Koobi Fora, but which may belong to different species (e.g., Alexeev, 1978; 1986; Walker and Leakey, 1978; Stringer, 1986; Chamberlain and Wood, 1987; Lieberman et al., 1988; 1996; Wood, 1991; 1992; Rightmire, 1993; Ferguson, 1995; Donnelly, 1996; Prat, 1997; 2004; Zeitoun, 2000). This could explain the apparition of this node in the trees of our analyses and raise the question: would this clade appear if we perform the same analyses exclusively using each specimen as representative of an OTU? The tree obtained with matrix A.1 (figure 4A) does not present the monophyletic clade associating *H. habilis* and *A. africanus* and would support the more traditional view of the inclusion of the *H. habilis* within the genus *Homo* (Prat, 2022). Another possible explanation for the formation of an *A. africanus*/*H. habilis* clade could be related to the anatomical region of the skull analysed here. Indeed, numerous morphological traits used to define *A. africanus* and *H. habilis* are based on facial and mandibular features (Rightmire, 1993; Prat, 1997; 2004; 2022), while the present study focuses exclusively on the calvarium, which is known to present less derived morphologies (e.g., Johanson et al., 1987; Rightmire, 1993; Prat, 1997; 2004; 2022), and could possibly explain the discrepancies in our results.

The constitution of a monophyletic group composed by the OTUs Sinanthropus-Sangiran-*H. georgicus*, with Sangiran and *H. georgicus* forming a terminal clade, also contributes to the current debates in palaeoanthropology. The occurrence of these two clades refers to the still unresolved argument about the definition of *H. erectus* as one or more species. Our results appear to support a possible exclusion of the Ngandong specimens from a *H. erectus* clade which would include all the *erectus*-like Eurasian OTUs (specimens from Dmanisi, Zoukoudian and Sangiran) to the exclusion of the African *erectus*-like OTUs (specimens from Koobi Fora). The above results, unlike the clade *A. africanus*/*H. habilis*, can be observed in all the trees with relatively high bootstrap values (from 51% to 55%) and are therefore better supported. It is important to note that the question of the attribution of the Ngandong sample (possibly together with the specimens from Sambungmacan) to the species *H. erectus* remains open to debate, with some authors classifying it as a distinct species: i.e., *H. soloensis* (Zeitoun, 2000; Durband, 2007; Tattersall and Schwartz, 2009; Zeitoun et al., 2010). Regarding the Dmanisi sample, it is interesting to note that they cluster with populations recognised as *H. erectus sensu stricto*

and are separate from African *H. erectus* or *H. ergaster*. These results are inconsistent with previous phenetic and phylogenetic interpretations of the Georgian hominin sample which underlined their morphological similarities with subcontemporary African fossils designated as *H. ergaster* (Rightmire et al., 2006; Lordkipanidze et al., 2013). In this new scenario, the Dmanisi, Sangiran and Zhoukoudian fossils could be grouped into a unique *H. erectus sensu stricto* species, different from both the African *H. ergaster* and the late Asian *H. erectus* such as Ngandong.

While the debate regarding the taxonomic position of *H. neanderthalensis* and *H. sapiens* has been somewhat fuelled by the recent genomic data indicating the existence of admixture between the two species (Green et al., 2010; Fu et al., 2015; Prüfer et al., 2021), most palaeoanthropologists now agree on the existence of two palaeoanthropologically valid species (e. g. Rak, 1993; Hublin, 2000; Harvati et al., 2004; White et al., 2014; Hajdinjak et al., 2018; Ni et al., 2021). However, the present study's results regarding *H. neanderthalensis* could question, yet again, the taxonomic status of this species: in all of our results, the Neanderthal and *H. sapiens* OTUs are not distinguished as two separate clades, suggesting that they could belong to one group. This phylogenetic result is in disagreement with recent cladistic studies based on discrete morphological features (Mounier and Caparros, 2015; Mounier and Mirazón Lahr, 2016) but is supported by numerous studies where Neanderthals and modern humans are considered variants of a same single species (e.g., Smith and Trinkaus, 1991; Trinkaus, 1991; Relethford, 2001; Ahern et al., 2002, 2004; Curnoe and Thorne, 2003).

There are a range of available interpretations that could explain such a result. First, the morphological differences between western and eastern populations of Neanderthals, as well as their relationship with *H. sapiens*, could be the consequences of a speciation by circular overlap or "ring species" (Voisin, 2006), i.e., "ring species provide dramatic evidence that normal genetic divergence within one species can build up to a sufficient level to generate two species" (Ridley, 2004:388). This would mean that "from Western Europe to the Near East, there was a succession of human populations that developed, over time, Neanderthal characters that became more and more marked from east to west; and in Western European Neanderthal populations, differentiation reached a level that did not allow interbreeding with modern humans. […] The farther those populations lived to the west, the more they displayed pronounced Neanderthal characters." (Voisin, 2006:311-318). However, it seems now unlikely that the classic Neanderthal populations would not have been able to interbreed with *H. sapiens* (Ahern et al., 2004; White et al., 2014 ; Prüfer et al., 2017; 2021).

Finally, the topology of our tree is consistent in clustering first the classic Neanderthals, followed by the early and Near East Neanderthals. This could be due to the more derived Neanderthal morphology observed in the late Western European Neanderthals (Dean et al., 1998; Condemi, 2001; Profico et al., 2023), while a less derived morphology would explain both the formation of the Near East and early Neanderthal clade in the first phylogenetic tree (i.e., Analysis A.1) and a possible stronger phylogenetic relationship with early *H. sapiens*.

An unequivocal interpretation of the results regarding *H. neanderthalensis* remains difficult at best, we cannot rule out that the use of different datasets could have had an impact on the building of the different phylogenetic hypotheses in this particular case. Additionally, most studies considering the phylogenetic and/or taxonomic status of *H. neanderthalensis* include other parts of the skull, such as the upper face and the mandible, where numerous specific Neanderthal features have been described (Hublin, 1998), and do not focus solely on the calvarium. Thus, we have to keep in mind that this region presents only a part of the total of morphological characteristics ("total morphological pattern") attributed to Neanderthals (e.g., Wood and Richmond, 2000; Smith et al., 2005; Tattersall and Schwartz, 2006).

Our results, while questioning the status of Neanderthals as they are grouped within a paraphyletic sequence, also raise the question of the status of the Ngandong specimens (see node J of figures 2-4), whose position in the phylogenies are a reminder of the proposed *H. sapiens soloensis* trinomial by Dubois (1940) and later taken up by several authors (Dubois, 1940; Campbell, 1963; Jelinek, 1981; Tobias, 1985; Stringer, 1987; Bonde, 1989; Bräuer and Mbua, 1992; Widianto and Zeitoun, 2003).

Regarding modern humans, in our results, they always form a monophyletic group, despite ambiguous relationships within the different populations of the species. It is important to note that *H. sapiens* are split in different OTUs representing relatively cohesive populations. This increases the morphological variation present in the database providing additional possibilities for the analysis to build phylogenetic hypotheses. In such a context, obtaining coherent and converging phylogenies, as is the case for the cladistic approaches developed in this study, advocates in favour of the reliability of the tested approach.

Finally, cladistics is concerned with the structure of phylogenetic relationships, while morphometry is a tool designed to describe morphology and shape which can be used in a phylogenetic framework (e.g., the reconstruction of ancestral shapes at nodes, Mounier and Mirazón Lahr, 2016; 2019).

To conclude on this point of reflection between interpretation and discussion on processes and taxonomy in the context of a phylogenetic analysis, let us recall that Tassy (1991) specifies that if the concept of phylogeny is conceived as the history of ruptures in the gene "pools" and the appearance of new "pools" isolated between populations, then we should indeed speak of tokogeny (Wheeler and Meier, 2000). This term describes infraspecific relationships according to Hennig (1966), who adds that relationships between terminal taxa are not necessarily hierarchical. Thus, if the aim of phylogeny is to put forward hypotheses

of relationships between units seen as recognisable, isolated and closed sets, these units may be species but not necessarily identical to the evolutionary units. They can be populations that may be reduced to a few individuals and not necessarily isolated from other populations of the species (Zeitoun, 2000).

Conclusions

In the present paper, we applied two protocols using geometric morphometric data in a cladistic framework on three different datasets, with the aim of testing the potential of such methodology. We obtained coherent results, describing possible phylogenetic and taxonomic hypotheses for the evolution of the genus *Homo* (i.e., a clade of *A. africanus*/*H. habilis*; a grouping of Sangiran/Sinanthropus/*H. georgicus* with the exclusion of Ngandong, paraphyly of Neanderthals and monophyly of *H. sapiens*). We are fully aware that caution is needed when it comes to interpreting such results. Many factors (i.e., the grouping of the OTUs, the anatomical region considered, the number and distribution of landmarks) could, indeed, contribute to shape the outcome of this kind of analysis and therefore the ability to understand the evolutionary mechanisms implied. Nevertheless, these results demonstrate the interest and potentiality of such an approach in palaeoanthropology, as they both confirm well-established ideas about the phylogeny of the genus *Homo* while bringing challenging ideas which can contribute to some of the most heated debates among paleoanthropologists today.

Acknowledgements

For permission to study specimens in their care, we thank directors and curators of the following institutions: Duckworth Laboratory, Cambridge; Distong National Museum of Natural History, Pretoria; Institut de Paléontologie Humaine, Paris; Musée de l'Homme, Paris; Museo di Antropologia, Sapienza Università di Roma; Museo Pigorini, Rome; National Museums of Kenya, Nairobi; ORSA database, Penn Museum; Peabody Museum, Cambridge; Senkenberg Forschungsinstiut und Naturmeseum, Frankfurt; and American Museum of Natural History, New York.

We thank K. Gerdau for the language proofing, Y. Heuzé, the Editor, and two anonymous reviewers for valuable comments and criticisms of earlier drafts that contributed to the improvement of this paper.

Finally, the program TNT is freely available, thanks to a subsidy from the Willi Hennig Society.

References

Abdi H, Williams LJ (2010) Principal component analysis. WIREs Computational Statistics 2(4):433-459 [https://doi.org/10.1002/wics.101]

Adams DC, Cardini A, Monteiro LR et al (2011) Morphometrics and phylogenetics: Principal components of shape from cranial modules are neither appropriate nor effective cladistic characters. Journal of Human Evolution 60(2):240-243 [https://doi.org/10.1016/j.jhevol.2010.02.003]

Ahern JCM, Karavanić I, Paunović M et al (2004) New discoveries and interpretations of hominid fossils and artifacts from Vindija Cave, Croatia. Journal of Human Evolution 46(1):27-67 [https://doi.org/10.1016/j.jhevol.2003.09.010]

Ahern JCM, Lee S-H, Hawks JD (2002) The late Neandertal supraorbital fossils from Vindija Cave, Croatia: A biased sample? Journal of Human Evolution 43(3):419-432 [https://doi.org/10.1006/jhev.2002.0586]

Alexeev VP (1978) Paleoantropologija Zemnogo šara i formirovanie čelovečeskih ras paleolit.

Alexeev VP (1986) The origin of the human race. Progress

Argue D (2017) *Homo rudolfensis*, 1-4 p [https://doi.org/10.1007/978-3-319-16999-6_3434-2]

Ascarrunz E, Claude J, Joyce WG (2019) Estimating the phylogeny of geoemydid turtles (Cryptodira) from landmark data: An assessment of different methods. PeerJ 7:e7476 [https://doi.org/10.7717/peerj.7476]

Ascarrunz E, Claude J, Joyce WG (2021) The phylogenetic relationships of geoemydid turtles from the Eocene Messel Pit Quarry: A first assessment using methods for continuous and discrete characters. PeerJ 9:e11805 [https://doi.org/10.7717/peerj.11805]

Balzeau A, Gilissen E, Grimaud-Hervé D (2012) Shared pattern of endocranial shape asymmetries among great apes, anatomically modern humans, and fossil Hominins. PLOS ONE 7(1): e29581 [https://doi.org/10.1371/journal.pone.0029581]

Black D (1927) On the lower molar hominid tooth from the Chou Kou Tien deposit. Paleontologica Sinica 7(D):1-28

Bonde N (1989) *Erectus* and *neanderthalensis* as species or subspecies of *Homo* with a model of speciation in hominids. In: Jiacomo E (ed) Hominidae. Jaca Book, Milan, pp 205-208

Bookstein FL (1989) Principal warps: Thin-plate splines and the decomposition of deformations. IEEE Transactions on Pattern Analysis and Machine Intelligence 11(6):567-585 [https://doi.org/10.1109/34.24792]

Bookstein FL (1994) Can biometrical shape be a homologous character? In: Hall BK (ed) Homology: The Hierarchial Basis of Comparative Biology. Academic Press, San Diego, pp 197-227

Bookstein FL (1997) Morphometric tools for landmark data: Geometry and biology, 1st Paperback ed., Cambridge University Press, Cambridge, 435 p

Bookstein FL (2002) Creases as morphometric characters. In MacLeod N, Forey PL (eds) Morphology, Shape and Phylogeny. Taylor & Francis, London, pp 139-174

Boule M (1911) L'homme fossile de La Chapelle-aux-Saints. Annales de Paléontologie 6:109-172

Boule M (1912) L'homme fossile de La Chapelle-aux-Saints. Annales de Paléontologie 7:105-192

Boule M (1913) L'homme fossile de La Chapelle-aux-Saints. Annales de Paléontologie 8:1-62

Bräuer G, Mbua E (1992) *Homo erectus* features used in cladistics and their variability in Asian and African hominids. Journal of Human Evolution 22(2):79-108 [https://doi.org/10.1016/0047-2484(92)90032-5]

Broca P (1868) Sur les crânes et ossements des Eyzies. Bulletins et Mémoires de la Société d'Anthropologie de Paris 30:335-349 [https://doi.org/10.3166/bmsap-2018-0027]

Catalano SA, Goloboff PA, Giannini NP (2010) Phylogenetic morphometrics (I): The use of landmark data in a phylogenetic framework. Cladistics 26(5):539-549 [https://doi.org/10.1111/j.1096-0031.2010.00302.x]

Campbell B (1963) Quantitative Taxonomy and Human Evolution. In: 1st Edition (ed) Classification and Human Evolution. Taylor and Francis, London, pp 50-75

Chamberlain AT, Wood BA (1987) Early hominid phylogeny. Journal of Human Evolution 16(1):119-133 [https://doi.org/10.1016/0047-2484(87)90063-7]

Clarke RJ (2008) Latest information on Sterkfontein's *Australopithecus* skeleton and a new look at *Australopithecus*: research in action. South African Journal of Science 104(11):443-449 [https://hdl.handle.net/10520/EJC96745]

Clouse RM, de Bivort BL, Giribet G (2011) Phylogenetic signal in morphometric data. Cladistics 27(4):337-340 [https://doi.org/10.1111/j.1096-0031.2010.00346.x]

Condemi S (1992) Les Hommes fossiles de Saccopastore et leurs relations phylogénétiques, CNRS, Paris, 174 p

Condemi S (2001) Les néandertaliens de La Chaise : Abri Bourgeois-Delaunay (Vol. 15), Comité des travaux historiques et scientifiques-CTHS, 178 p

Curnoe D, Thorne A (2003) Number of ancestral human species: A molecular perspective. HOMO 53(3):201-224 [https://doi.org/10.1078/0018-442X-00051]

Dart RA (1925) *Australopithecus africanus* The Man-Ape of South Africa. Nature 115(2884) [https://doi.org/10.1038/115195a0]

Dean D, Hublin J-J, Holloway R et al (1998) On the phylogenetic position of the pre-Neandertal specimen from Reilingen, Germany. Journal of Human Evolution 34(5):485-508 [https://doi.org/10.1006/jhev.1998.0214]

Donnelly SM (1996) How different are KNM-ER 1470 and KNM-ER 1813? A multivariate comparison using randomization methods. American Journal of Physical Anthropology Suppl.(22):99

Dubois E (1893) Palaeontologische onderzoekingen op Java. Verslag van Het Mijnwezen Batavia 10:10-14

Dubois E (1894) Palaeontologische onderzoekingen op Java. Verslag van Het Mijnwezen Batavia 4:14-18

Dubois E (1940) The fossil human remains discovered in Java by Dr. G.H.R. von Koenigswald and attribuated by him to *Pithecanthropus erectus*, in reality remains of *Homo sapiens soloensis*. Nederlandse Akademie van Wetenschappen 43:841-854

Durband AC (2007) The view from down under: a test of the multiregional hypothesis of Modern Human origins using the basicranial evidence from Australasia. Coll. Antropol 31(3): 651-659

Fabre V, Condemi S, Degioanni A (2009) Genetic evidence of geographical groups among Neanderthals. PLOS ONE 4(4): e5151 [https://doi.org/10.1371/journal.pone.0005151]

Farris JS (1989) The retention index and the rescaled consistency index. Cladistics: The International Journal of the Willi Hennig Society 5(4):417-419 [https://doi.org/10.1111/j.1096-0031.1989.tb00573.x]

Felsenstein J (1985) Confidence limits on phylogenies: An approach using the bootstrap. Evolution; International Journal of Organic Evolution 39(4):783-791 [https://doi.org/10.1111/j.1558-5646.1985.tb00420.x]

Felsenstein J (2004) Inferring Phylogenies, Sinauer Associates, Sunderland, 580 p

Ferguson WW (1995) A new species of the genus *Homo* (primates: Hominidae) from the Plio/Pleistocene of Koobi Fora, in Kenya. Primates 36(1):69-89 [https://doi.org/10.1007/BF02381916]

Fu Q, Hajdinjak M, Moldovan OT et al (2015) An early modern human from Romania with a recent Neanderthal ancestor. Nature 524(7564):216-219 [https://doi.org/10.1038/nature14558]

Gabounia L, de Lumley M-A, Vekua A et al (2002) Découverte d'un nouvel hominidé à Dmanissi (Transcaucasie, Géorgie). Comptes Rendus Palevol 1(4):243-253 [https://doi.org/10.1016/S1631-0683(02)00032-5]

Goloboff PA, Catalano SA (2011) Phylogenetic morphometrics (II): Algorithms for landmark optimization. Cladistics 27(1):42-51 [https://doi.org/10.1111/j.1096-0031.2010.00318.x]

Goloboff PA, Catalano SA (2016) TNT version 1.5, including a full implementation of phylogenetic morphometrics. Cladistics 32 (3):221-238 [https://doi.org/10.1111/cla.12160]

Goloboff PA, Farris JS, Nixon KC (2008) TNT, a free program for phylogenetic analysis. Cladistics 24(5):774-786 [https://doi.org/10.1111/j.1096-0031.2008.00217.x]

González-José R, Escapa I, Neves WA et al (2008) Cladistic analysis of continuous modularized traits provides phylogenetic signals in *Homo* evolution. Nature 453(7196):775-778 [https://doi.org/10.1038/nature06891]

González-José R, Escapa I, Neves WA et al (2011) Morphometric variables can be analyzed using cladistic methods: A reply to Adams et al. Journal of Human Evolution 60(2):244-245 [https://doi.org/10.1016/j.jhevol.2010.11.001]

Goodall C (1991) Procrustes methods in the statistical analysis of shape. Journal of the Royal Statistical Society: Series B (Methodological) 53(2):285-321 [https://doi.org/10.1111/j.2517-6161.1991.tb01825.x]

Gower JC (1975) Generalized procrustes analysis. Psychometrika 40(1):33-51 [https://doi.org/10.1007/bf02291478]

Gray JE (1825) An outline of attempt at the disposition of Mammalian into tribes and families with a list of the genera apparently appertaining to each tribe. Annals of Philosophy 10: 337-344

Green RE, Krause J, Briggs AW et al (2010) A draft sequence of the Neandertal genome. Science 328(5979):710-722 [https://doi.org/10.1126/science.1188021]

Grimaud D (1982) Évolution du pariétal de l'homme fossile. Position de l'Homme de Tautavel parmi les hominidés, Thèse Géologie des formations sédimentaires option Préhistoire, Université de Provence, Aix-Marseille, 705 p

Grine FE, Jungers WL, Schultz J (1996) Phenetic affinities among early *Homo* crania from East and South Africa. Journal of Human Evolution 30(3):189-225 [https://doi.org/10.1006/jhev.1996.0019]

Groves CP (1989) Theory of human and primate evolution, Clarendon Press, 384 p

Groves CP, Mazák V (1975) An approach to the taxonomy of the Hominidae: Gracile Villafranchian hominids of Africa. Casopis pro Mineralogii a Geologii 20:225-247

Hajdinjak M, Fu Q, Hübner A, et al (2018) Reconstructing the genetic history of late Neanderthals. Nature 555(7698):652-656 [https://doi.org/10.1038/nature26151]

Harvati K, Frost SR, McNulty KP (2004) Neanderthal taxonomy reconsidered: Implications of 3D primate models of intra- and interspecific differences. Proceedings of the National Academy of Sciences 101(5):1147-1152 [https://doi.org/10.1073/pnas.0308085100]

Hennig W (1966) Phylogenetic Systematics, University of Illinois Press, Urbana, 587 p [https://doi.org/10.1146/annurev.en.10.010165.000525]

Hublin J-J (1998) Climatic changes, paleogeography, and the evolution of the Neandertals. In: Akazawa T, Aoki K, Bar-Yosef O (eds) Neandertals and Modern Humans in Western Asia. Springer US, pp 295-310 [https://doi.org/10.1007/0-306-47153-1_18]

Hublin J-J (2000) Modern-nonmodern hominid interactions: A mediterranean perspective. In: Bar-Yosef O, Pilbeam D (eds) The geography of the neandertals and modern humans in Europe and the greater Mediterranean, Harvard Peabody Museum, Cambridge, pp 157-182

Jelinek J (1981) Was *Homo erectus* already *Homo sapiens*? In: Ferembach D (ed) Les processus de l'hominisation. CNRS Éditions, pp 85-89

Johanson DC, Masao FT, Eck GG et al (1987) New partial skeleton of *Homo habilis* from Olduvai Gorge, Tanzania. Nature 327 (6119):205-209 [https://doi.org/10.1038/327205a0]

King W (1864) The reputed fossil man of the Neanderthal. Quaterly Journal of Science 1:88-97

Klingenberg CP, Barluenga M, Meyer A (2002) Shape analysis of symmetric structures: Quantifying variation among individuals and asymmetry. Evolution 56(10):1909-1920 [https://doi.org/10.1111/j.0014-3820.2002.tb00117.x]

Klingenberg CP, Gidaszewski NA (2010) Testing and quantifying phylogenetic signals and homoplasy in morphometric data. Systematic Biology 59(3):245-261 [https://doi.org/10.1093/sysbio/syp106]

Koenigswald GHR (1940) Neue Pithecanthropus-Funde 1936-1938: Ein Beitrag zur Kenntnis der Praehominiden, Landsdrukkerij, Batavia, 232 p

Leakey LSB, Tobias PV, Napier JR (1964) A new species of the genus *Homo* from Olduvai Gorge. Nature 202(4927) [https://doi.org/10.1038/202007a0]

Lieberman DE, Pilbeam DR, Wood BA (1988) A probabilistic approach to the problem of sexual dimorphism in *Homo habilis*: A comparison of KNM-ER 1470 and KNM-ER 1813. Journal of Human Evolution 17(5):503-511 [https://doi.org/10.1016/0047-2484(88)90039-5]

Lieberman DE, Wood BA, Pilbeam DR (1996) Homoplasy and early *Homo*: An analysis of the evolutionary relationships of *H. habilis sensu stricto* and *H. rudolfensis*. Journal of Human Evolution 30(2):97-120 [https://doi.org/10.1006/jhev.1996.0008]

Lockwood CA, Tobias PV (1999) A large male hominin cranium from Sterkfontein, South Africa, and the status of *Australopithecus africanus*. Journal of Human Evolution 36 (6):637-685 [https://doi.org/10.1006/jhev.1999.0299]

Lordkipanidze D, Ponce de León MS, Margvelashvili A et al (2013) A complete skull from Dmanisi, Georgia, and the Evolutionary Biology of Early *Homo*. Science 342(6156):326-331 [https://doi.org/10.1126/science.1238484]

MacLeod N, Forey PL, Systematics Association (2002) Morphology, shape and phylogeny, Taylor & Francis, London, 318 p

MacLeod N, Forey PL (2002) Phylogenetic signals in morphometric data. In: MacLeod N, Forey PL (eds) Morphology, shape and phylogeny. Taylor & Francis, London, pp 100-138

Matile L, Tassy P, Goujet D (1987) Introduction à la systématique zoologique (concepts, principes, méthodes), Société française de systématique, Paris, 126 p

Monteiro LR (2000) Why Morphometrics is Special: The problem with using partial warps as characters for phylogenetic inference. Systematic Biology 49(4):796-800

Mounier A (2012) Le massif facial supérieur d'*Homo heidelbergensis* Schoetensack, 1908 : l'apport de la morphométrie géométrique. Bulletins et Mémoires de la Société d'Anthropologie de Paris 24(1):51-68 [https://doi.org/10.1007/s13219-011-0041-3]

Mounier A, Caparros M (2015) The phylogenetic status of *Homo heidelbergensis* – a cladistic study of Middle Pleistocene hominins. Bulletins et Mémoires de la Société d'Anthropologie de Paris 27(3-4):110-134 [https://doi.org/10.1007/s13219-015-0127-4]

Mounier A, Condemi S, Manzi G (2011) The stem species of our species: A place for the archaic human cranium from Ceprano, Italy. PLOS ONE 6(4):e18821 [https://doi.org/10.1371/journal.pone.0018821]

Mounier A, Marchal F, Condemi S (2009) Is *Homo heidelbergensis* a distinct species? New insight on the Mauer mandible. Journal of Human Evolution 56(3):219-246 [https://doi.org/10.1016/j.jhevol.2008.12.006]

Mounier A, Mirazón Lahr M (2016) Virtual ancestor reconstruction: revealing the ancestor of modern humans and Neandertals. Journal of Human Evolution 91:57-72 [https://doi.org/10.1016/j.jhevol.2015.11.002]

Mounier A, Mirazón Lahr M (2019) Deciphering African late middle Pleistocene hominin diversity and the origin of our species. Nature Communications 10(1) [https://doi.org/10.1038/s41467-019-11213-w]

Ni X, Ji Q, Wu W et al (2021) Massive cranium from Harbin in northeastern China establishes a new Middle Pleistocene human lineage. The Innovation 2(3):100130 [https://doi.org/10.1016/j.xinn.2021.100130]

Olivier G (1960) Pratique anthropologique, Vigot Frères, Paris, 299 p

Oppenoorth WFF (1932) *Homo (javanthropus) soloensis*, en Plistocene mensch van Java. Wetenschappelijke Medische Dienst Mijnbouw Nederlandsch Indië 20:49-74

Prat S (1997) Problème taxinomique des premiers représentants du genre Homo. Études crâniennes des individus d'Olduvai et de Koobi Fora. Bulletins et Mémoires de la Société d'Anthropologie de Paris 9(3):251-266 [https://doi.org/10.3406/bmsap.1997.2484]

Prat S (2004) Les premiers représentants du genre *Homo*, en quête d'une identité. Apports de l'étude morphologique et de l'analyse cladistique. Bulletins et Mémoires de la Société d'Anthropologie de Paris 16(1-2):17-35 [https://doi.org/10.4000/bmsap.586]

Prat S (2022) Emergence of the genus *Homo*: From concept to taxonomy. L'Anthropologie 126(4):103068 [https://doi.org/10.1016/j.anthro.2022.103068]

Profico A, Buzi C, Di Vincenzo F et al (2023) Virtual excavation and analysis of the early Neanderthal cranium from Altamura (Italy). Communications Biology 6(1) [https://doi.org/10.1038/s42003-023-04644-1]

Profico A, Di Vincenzo F, Gagliardi L et al (2016) Filling the gap. Human cranial remains from Gombore II (Melka Kunture, Ethiopia; ca. 850 ka) and the origin of *Homo heidelbergensis*. Journal of Anthropological Sciences 94:41-63 [https://doi.org/10.4436/JASS.94019]

Prüfer K, de Filippo C, Grote S et al (2017) A high-coverage Neandertal genome from Vindija Cave in Croatia. Science 358 (6363):655-658 [https://doi.org/10.1126/science.aao1887]

Prüfer K, Posth C, Yu H et al (2021) A genome sequence from a modern human skull over 45,000 years old from Zlatý kůň in Czechia. Nature Ecology & Evolution 5(6):820-825 [https://doi.org/10.1038/s41559-021-01443-x]

Rak Y (1993) Morphological variation in *Homo neanderthalensis* and *Homo sapiens* in the Levant. In: Kimbel WH, Martin LB (eds) Species, species concepts and primate evolution. Springer US, Boston, pp 523-536 [https://doi.org/10.1007/978-1-4899-3745-2_20]

Relethford JH (2001) Absence of regional affinities of Neandertal DNA with living humans does not reject multiregional evolution. American Journal of Physical Anthropology 115(1):95-98 [https://doi.org/10.1002/ajpa.1060]

Ridley M (2004) Evolution, 3rd Edition, Wiley-Blackwell, Wiley, 800 p

Rightmire GP (1993) Variation among early *Homo* crania from Olduvai Gorge and the Koobi Fora region. American Journal of Physical Anthropology 90(1):1-33 [https://doi.org/10.1002/ajpa.1330900102]

Rightmire GP, Lordkipanidze D, Vekua A (2006) Anatomical descriptions, comparative studies and evolutionary significance of the hominin skulls from Dmanisi, Republic of Georgia. Journal of Human Evolution 50(2):115-141 [https://doi.org/10.1016/j.jhevol.2005.07.009]

Rohlf FJ (1998) On applications of geometric morphometrics to studies of ontogeny and phylogeny. Systematic Biology 47 (1):147-158

Rohlf FJ, Slice D (1990) Extensions of the procrustes method for the optimal superimposition of landmarks. Systematic Biology 39(1):40-59 [https://doi.org/10.2307/2992207]

Sartono S (1982) Characteristics and chronology of early men in Java. In: de Lumley H (ed) *Homo erectus* et la place de l'Homme de Tautavel parmi les Hominidés fossiles. Premier Congrès International de Paléontologie Humaine, pp 491-541

Smith FH, Janković I, Karavanić I (2005) The assimilation model, modern human origins in Europe, and the extinction of Neandertals. Quaternary International 137(1):7-19 [https://doi.org/10.1016/j.quaint.2004.11.016]

Smith FH, Trinkaus E (1991) Les origines de l'homme moderne en Europe centrale : un cas de continuité. In: Hublin J-J, Tillier AM (eds) Aux origines d'*Homo sapiens*. Press universitaires de France, Paris, pp 251-290

Smith UE, Hendricks JR (2013) Geometric morphometric character suites as phylogenetic data: extracting phylogenetic signal from Gastropod shells. Systematic Biology 62(3):366-385 [https://doi.org/10.1093/sysbio/syt002]

Sneath PHA, Sokal RR (1973) Numerical taxonomy. The principles and practice of numerical classification, W.H. Freeman and Co., 573 p

Stringer CB (1986) The credibility of *Homo habilis*. In: Wood B, Martin L, Andrews P (eds) Major topics in primate and human evolution. Cambridge University Press, Cambridge, pp 266-294

Stringer CB (1987) A numerical cladistic analysis for the genus *Homo*. Journal of Human Evolution 16(1):135-146 [https://doi.org/10.1016/0047-2484(87)90064-9]

Swofford D, Olsen GJ, Waddell PJ, Hillis DM (1996) Phylogenetic Inference. In: Hillis DM, Moritz C, Mable BK (eds) Molecular Systematics, 2nd Edition. Sinauer Associates, Sunderland, pp 407-514

Tassy P (1991) L'arbre à remonter le temps. Les rencontres de la systématique et de l'évolution, C. Bourgeois, Paris, p 455

Tattersall I (2013) *Homo ergaster* and its contemporaries. In: Henke W, Tattersall I (eds) Handbook of Paleoanthropology. Springer, Berlin, pp 1-18 [https://doi.org/10.1007/978-3-642-27800-6_53-5]

Tattersall I, Schwartz JH (2006) The distinctiveness and systematic context of *Homo neanderthalensis*. In: Hublin J-J, Harvati K, Harrison T (eds) Neanderthals revisited: new approaches and perspectives. Springer, Netherlands, pp 9-22 [https://doi.org/10.1007/978-1-4020-5121-0_2]

Tattersall I, Schwartz JH (2009) Evolution of the Genus *Homo*. Annual Review of Earth and Planetary Sciences 37(1):67-92 [https://doi.org/10.1146/annurev.earth.031208.100202]

Thiele K (1993) The Holy grail of the perfect character: The cladistic treatment of mophometric data. Cladistics 9(3):275-304 [https://doi.org/10.1111/j.1096-0031.1993.tb00226.x]

Tobias PV (1980) '*Australopithecus afarensis*' and *A. africanus*: Critique and alternative hypothesis. Palaeontologica Africana 23:1-17

Tobias PV (1985) Single characters and total morphological pattern redefined the sorting effected by a selection of morphological features of the early hominids. In: Delson E (ed) Ancestors: The Hard Evidence. A.R. Liss, Michigan, pp 94-101

Torres A, Goloboff PA, Catalano SA (2022) Parsimony analysis of phylogenomic datasets (I): Scripts and guidelines for using TNT (Tree Analysis using New Technology). Cladistics 38 (1):103-125 [https://doi.org/10.1111/cla.12477]

Trinkaus E (1991) Les Hommes fossiles de la grotte de Shanidar, Irak : Évolution et continuité parmi les Hommes archaïques et tardifs du Proche-Orient. L'Anthropologie 95(2-3):535-572

Vandermeersch B (1981) Les Hommes de Qafzeh (Israël), CNRS, Paris, p 319

Villmoare B, Kimbel WH, Seyoum C et al (2015) Early *Homo* at 2.8 Ma from Ledi-Geraru, Afar, Ethiopia. Science 347(6228): 1352-1355 [https://doi.org/10.1126/science.aaa1343]

Voisin JL (2006) Speciation by distance and temporal overlap: A new approach to understanding Neanderthal evolution. In: Hublin J-J, Harvati K, Harrison T (eds) Neanderthals revisited: new approaches and perspectives. Springer, Netherlands, pp 299-314 [https://doi.org/10.1007/978-1-4020-5121-0_17]

Walker A, Leakey REF (1978) The Hominids of East Turkana. Scientific American 239(2):54-67

Walker A, Leakey REF (1993) The Nariokotome *Homo Erectus* Skeleton. Harvard University Press, Cambridge, Massachusetts, p 482

Wheeler QD, Meier R (2000) Species concepts and phylogenetic theory: a debate. Columbia University Press, New York, p 245

White S, Gowlett JAJ, Grove M (2014) The place of the Neanderthals in hominin phylogeny. Journal of Anthropological Archaeology 35:32-50 [https://doi.org/10.1016/j.jaa.2014.04.004]

White TD, Johanson DC, Kimbel WH (1981) *Australopithecus africanus*: its phyletic position reconsidered. South African Journal of Science 77:445-470

Widianto H, Zeitoun V (2003) Morphological description, biometry and phylogenetic position of the skull of Ngawi 1 (east Java, Indonesia). International Journal of Osteoarchaeology 13(6): 339-351 [https://doi.org/10.1002/oa.694]

Wiley DF (2005) *Landmark* (3.0). IDAV, University of California, Davis

Wood B (1991) Koobi Fora research project: researches into geology, palaeontology, and human origins. Volume 4. Hominid cranial remains. Clarendon Press, Oxford, p 632

Wood B (1992) Origin and evolution of the genus *Homo*. Nature 355 (6363) [https://doi.org/10.1038/355783a0]

Wood B, Collard M (1999) The Human Genus. Science 284 (5411):65-71 [https://doi.org/10.1126/science.284.5411.65]

Wood B, Richmond BG (2000) Human evolution: taxonomy and paleobiology. The Journal of Anatomy 197(1):19-60 [https://doi.org/10.1046/j.1469-7580.2000.19710019.x]

Zeitoun V (2000) Révision de l'espèce *Homo erectus* (Dubois, 1893). Bulletins et Mémoires de la Société d'Anthropologie de Paris 12(1-2) [https://doi.org/10.4000/bmsap.5963]

Zeitoun V, Détroit F, Grimaud-Hervé D, Widianto H (2010) Solo man in question: Convergent views to split Indonesian *Homo erectus* in two categories. Quaternary International 223-224: 281-292 [https://doi.org/10.1016/j.quaint.2010.01.018]

Zelditch ML, Fink WL, Swiderski DL (1995) Morphometrics, homology, and phylogenetics: Quantified characters as synapomorphies. Systematic Biology 44(2):179-189 [https://doi.org/10.1093/sysbio/44.2.179]

Zelditch ML, Swiderski DL, Fink WL (2000) Discovery or phylogenetic characters in morphometric data. In: Wiens JJ (ed) Phylogenetic analysis of morphological data. Smithsonian Institution Press, Washington DC, pp 37-83

Zelditch ML, Swiderski DL, Sheets HD (2004) Geometric morphometrics for biologists: A primer, Academic Press, p 488